Tribol Lett (2010) 40:247–268
DOI 10.1007/s11249-010-9671-8

ORIGINAL PAPER

# A Review of Ionic Liquids for Green Molecular Lubrication in Nanotechnology

**Manuel Palacio · Bharat Bhushan**

Received: 19 April 2010 / Accepted: 13 July 2010 / Published online: 27 July 2010


**Abstract** Common industrial lubricants include natural and synthetic hydrocarbons and perfluoropolyethers (PFPEs), where the latter is widely used in commercial applications requiring extreme operating conditions due to their high temperature stability and extremely low vapor pressure. However, PFPEs exhibit low electrical conductivity, making them undesirable in some nanotechnology applications. Ionic liquids (ILs) have been explored as lubricants for various device applications due to their excellent electrical conductivity as well as good thermal conductivity, where the latter allows frictional heating dissipation. Since they do not emit volatile organic compounds, they are regarded as "green" lubricants. In this article, we review the different types of ILs and their physical properties responsible for lubrication. We also discuss their suitability as lubricants, since the long-term performance of ILs as lubricants may be affected by issues such as corrosion, oxidation, tribochemical reactions, and toxicity. We present nanotribological, electrical, and spectroscopic studies of IL films along with conventional tribological investigations, recognizing that understanding the tribological performance at various length scales is a crucial step in selecting and designing effective lubricants.

**Keywords** Ionic liquids · Friction · Wear · Tribochemical reactions · Corrosion · Oxidation

M. Palacio · B. Bhushan (✉)
Nanoprobe Laboratory for Bio- & Nanotechnology and Biomimetics, The Ohio State University, Columbus, OH 43210, USA
e-mail: Bhushan.2@osu.edu

## 1 Introduction

Advances in nanotechnology have resulted in the development of new materials and devices, which contain features in the micron and nanometer scales, and require interfaces possessing low adhesion, friction, and wear. Examples of the commercial nanotechnological applications that have been developed over the past two decades where micro-/nanoscale tribological performance is important include magnetic hard disks, magnetic tapes, micro-/nanoelectromechanical systems (MEMS/NEMS), the micromirror components of commercial digital light processing (DLP) equipment, and the drive mechanism of the green laser used in microprojectors [1–7]. For example, adhesion is the major cause of the failure of accelerometers used in automobile air bag triggering mechanisms and the micromirrors in the DLP [8–10]. Wear has been found to compromise the performance of NEMS-based atomic force microscopy (AFM) data storage systems [11, 12].

In order to improve tribological performance, liquid lubricants are applied onto the surfaces of the devices mentioned above. The ideal liquid lubricant should be molecularly thick, easily applied, able to chemically bond to the micro/nanodevice surface, insensitive to environment, and highly durable [13–15].

### 1.1 Lubricant Types

Traditionally, liquid lubricants are classified as either natural organic or synthetic organic [1, 4]. Natural organic lubricants include commonly used oils such as animal fats, shark oil, whale oil, mineral oils, and vegetable oils. Mineral (or petroleum) oils, which include straight paraffin, branched paraffin, naphthene, and aromatic oils, are the most widely used lubricants in this category.

Synthetic organic lubricants were initially developed in response to the needs of the aviation industry for lubricants that are capable of withstanding greater temperature extremes. The main classes of synthetic lubricants include synthetic hydrocarbons, chlorofluorocarbons, esters, silicones, silanes, polyphenyl ethers (PPE), and perfluoropolyethers (PFPEs). PFPEs are among the most widely used synthetic organic lubricant for applications requiring extreme operating conditions due to its high temperature stability and extremely low vapor pressure. The major applications of PFPEs are as oils for high-vacuum applications, hydraulic fluids, gas turbine engine oils, and magnetic hard disks and tapes [1].

### 1.2 Ionic Liquids

Ionic liquids (ILs), of more recent interest, and the main focus of this article, are synthetic liquids that contain a positive ion (cation) and a negative ion (anion), where one or both of the ions are organic compounds [16, 17]. The ILs were initially developed for use as electrolytes in batteries and for electrodeposition [16, 18]. However, recent applications have geared these compounds as environmentally friendly solvents for chemical synthesis ("green chemistry") where these liquids are used as substitutes for conventional organic solvents. Other applications include supercritical fluids, active pharmaceutical ingredients, as well as heat transfer fluids [18–21]. ILs have been investigated over the last decade for lubrication applications [17, 22–32]. Similar to PFPEs, ILs exhibit high temperature stability, low vapor pressure, and desirable lubrication properties. The main difference between PFPEs and ILs is that while the former is electrically insulating, the latter can be considered as electrically conducting. Relative to PFPEs, the higher thermal conductivity of ILs enables them to dissipate heat during sliding more effectively [33, 34]. This correlation between the electrical and thermal conductivities is analogous to the Wiedemann–Franz law for metals [35]. ILs do not emit volatile organic compounds, making them "green" lubricants. From the commercial standpoint, some of the common ILs are cheaper than PFPEs by a factor of two or so, providing further motivation for evaluating the suitability of ILs as lubricants. However, there are potential disadvantages on the use of ILs as lubricants, such as their potential to corrode the substrate (the material that the lubricants are applied to), as well as the formation of decomposition by-products that could be corrosive, flammable or toxic. A list of the advantages and disadvantages on the use of ILs as lubricants is presented in Table 1.

### 1.3 Objectives

The objectives of this article are as follows. The first main objective is to review the chemical composition and physical properties of ILs, and discuss their suitability as lubricants. The second main objective is to review selected tribological and electrical studies performed at macro- to nanoscales, which, in combination with spectroscopic analysis, lead to proposed lubrication mechanisms for IL lubrication.

## 2 Background on ILs

In this section, we describe the composition and properties of ILs, and discuss their advantages and disadvantages as lubricants.

### 2.1 Composition of ILs

An IL is a synthetic salt with a melting point below 100 °C. A room temperature ionic liquid (RTIL) is a synthetic molten salt with melting points at or below room

**Table 1** List of advantages and disadvantages of ionic liquids as lubricants

| Advantages | Disadvantages |
|---|---|
| Customization of chemical and physical properties through selection of cation and anion | Research on tribological properties is very diffused due to the diversity of available ILs |
| Some ILs (esp. those with hydrophobic anions) are chemically stable | Some ILs are moisture-sensitive, leading to potential decomposition issues |
| Low vapor pressure prevents the emission of toxic fumes | Generation of toxic by-products (esp. ILs with halogen anions) may corrode surface |
| Most ILs are non-flammable | Some decomposition products generated during heating may be flammable or combustible |
| ILs do not emit volatile organic compounds ("green" lubricants) | Environmental toxicity of ILs still largely unknown |
| Electrically conductive | |
| High thermal conductivity | |
| Low cost compared to conventional synthetic organic lubricants | |

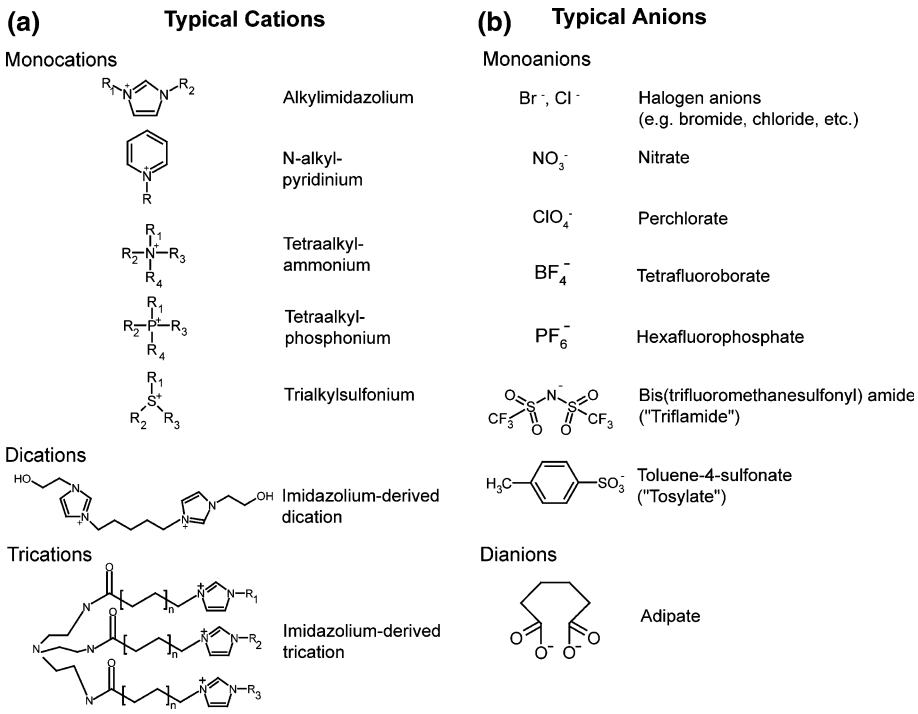


**Fig. 1** Chemical structures of common monovalent, divalent, and trivalent IL cations, and common monovalent and divalent IL anions

temperature. One or both of the ions are organic species. At least one ion has a delocalized charge such that the formation of a stable crystal lattice is prevented, and the ions are held together by strong electrostatic forces. As a result of the poor coordination of the ions, these compounds are liquid below 100 °C or even at room temperature [27].

### *2.1.1 Cations*

The number of combinations of anions and cations, which can be used to produce ILs, is in the range of one million. Typical cations, the general structures of which are shown in Fig. 1a, include imidazolium, pyridinium, ammonium, phosphonium, and sulfonium ions. In Fig. 1a, R stands for an organic group [34, 36]. It should be noted that the organic substituents are usually different from each other, i.e., $R_1 \neq R_2 \neq R_3 \neq R_4$, further increasing the potential number of available IL cations. To further illustrate the diversity of potential cations, examples of dications and trications are also shown in Fig. 1a. Compounds containing dications and trications have two and three anions, respectively, in order to maintain electrical neutrality. The presence of repeat units in the multivalent cations will affect its interactions with the substrate, and hence the tribological performance of the IL as a whole.

### *2.1.2 Anions*

Typical anions are shown in Fig. 1b. It includes the halogen anions, nitrate, perchlorate, tetrafluoroborate, hexafluorophosphate, *bis*(trifluoromethanesulfonyl) amide ("triflamide"), and toluene-4-sulfonate ("tosylate") [17, 34]. Anions can also be multivalent. The anions are usually classified based whether the anion tends to be hydrophilic or hydrophobic. This will greatly affect the tendency of the IL to form bonds to the substrate that it is deposited on, as well as its propensity for chemical reactions such as hydrolysis. For instance, hydrophilic anions such as $BF_4^-$ and $PF_6^-$ have a greater tendency to react with the substrate (for example, in metals and ceramics with surface active oxides and hydroxyl groups), but these anions also tend to be susceptible to chemical degradation reactions [31]. Therefore, the properties of the anion can greatly influence the tribological performance of the IL.

## 2.2 Properties of ILs

As an example, Table 2 lists the physical, thermal, and electrical properties of a commercially available IL, 1-butyl-3-methylimidazolium hexafluorophosphate, and its properties are compared to the PFPE lubricant Z-TETRAOL [27]. Both liquids can be regarded as high-performance liquids, having extremely low vapor pressures, high viscosity and suitability for extreme thermal conditions (both liquids decompose at $\sim$300 °C and above). The electrical conductivity (or resistivity) is the main property that distinguishes the two liquids. Unlike conventional lubricants that are electrically insulating, ILs can minimize the contact resistance between sliding surfaces because they are electrically conducting, making them suitable

**Table 2** Physical, thermal, and electrical properties of BMIM-$PF_6$ and Z-TETRAOL

| | 1-Butyl-3-methylimidazolium hexafluorophosphate (BMIM-$PF_6$) | Z-TETRAOL |
|---|---|---|
| Cation | $C_8H_{15}N_2^+$ | – |
| Anion | $PF_6^-$ | – |
| Molecular weight (g/mol) | 284[a] | 2300[b] |
| $T_{melting}$ (°C) | 10[c] | – |
| $T_{decomposition}$ (°C) | 300[c] | ~320[b] |
| Density (g/cm$^3$) | 1.37[a] | 1.75[b] |
| Kinematic | 281[a] (20 °C) | 2000[b] (20 °C) |
| Viscosity (mm$^2$/s) | 78.7[d] (40 °C) | |
| Pour point (°C) | <−50[e] | −67[b] |
| Specific heat (J/g K) | 1.44[f] (25 °C) | ~0.20[b] (50 °C) |
| Thermal conductivity at 25 °C (W/m K) | 0.15[g] | ~0.09[b] |
| Dielectric strength at 25 °C (kV/mm) | – | ~30[b] |
| Volume resistivity (Ω cm) | 714[h] | ~$10^{13}$ [b] |
| Vapor pressure at 20 °C (Torr) | <$10^{-9}$ | 5 × $10^{-7}$ [b] |
| Wettability on Si | Moderate[c] | – |
| Water contact angle on Si | 46° (untreated) | 54° (untreated) |
| | 39° (partially bonded) | 83° (partially bonded) |
| | 41° (fully bonded) | 88° (fully bonded) |
| Miscibility with isopropanol | Total[a] | – |
| Miscibility with water | None[h] | – |

[a] [37]
[b] [38]
[c] [34]
[d] [39]
[e] [40]
[f] [41]
[g] [42]
[h] [43]

lubricants for various electrical applications [12]. These liquids can also be used to mitigate arcing, which is a cause of electrical breakdown in sliding electrical contacts. In addition, ILs have high thermal conductivity which helps to dissipate heat during sliding [33]. As shown in Table 2, the specific heat (and to an extent, the thermal conductivity) of the IL is much better than the PFPE.

### 2.3 Lubrication Mechanisms of ILs

Aside from the physical properties described above, ILs present a unique combination of characteristics which make them attractive as lubricants for various material sliding pairs. In the boundary lubrication regime, where a thin lubricant film is present, the polar nature of ILs facilitates physical adsorption. This is known to be the main mechanism for the observed low friction and wear during the sliding of metal–metal, metal–ceramic, and ceramic–ceramic pairs under moderate sliding conditions [1, 3–5]. Under harsh sliding conditions, some IL anions have the tendency to decompose leading to the formation of scratch-resistant surface films such as $B_2O_3$, BN, $FeF_2$, and $FeF_3$ [22–24, 44]. In instances where the surface is reactive (e.g., Mg alloys, silica surfaces), the anions in ILs can exhibit stronger chemical adsorption interactions with the available ions and other surface active groups such as oxides and hydroxides, or the IL could decompose, with the new species forming surface films [29, 45].

In polymers, it has been shown that ILs can act as suitable lubricants as well. ILs have been shown to reduce the coefficient of friction and wear of polyamide 6 (PA 6) when applied either topically or mixed with PA 6 pellets during the injection molding process [46]. In the latter case, the mixing of the IL with the bulk PA 6 led to a decrease in the glass transition temperature of the polymer. The observed improvement in tribological properties (relative to PA 6 with no added IL) was attributed to the IL plasticizing the polymer during processing. In polymer–ceramic nanoparticle composites, the addition of ILs affects the morphology and agglomeration tendency of the nanoparticles, which then lead to the decrease in friction and wear on the surface [47].

Ionic liquids can also reduce friction and wear in the hydrodynamic and mixed hydrodynamic/boundary lubrication regimes. When used as additive to water for the lubrication of silicon nitride surfaces, certain ILs have been shown to minimize wear by reducing the running-in period. The presence of the IL may promote the creation of an electric double layer, formed by the negatively charged $Si_3N_4$ surface attracting the IL cations to the deposit on the surface. The electric double layer can lead to a reduction of the coefficient of friction due to an improvement in the load carrying capacity of the lubricant [25, 48].

### 2.4 Issues on the Applicability of ILs as Lubricants

The main issues concerning the suitability of ILs as lubricants are the following: IL causing corrosion on the substrate surface, oxidation of the IL, the occurrence of tribochemical reactions at the sliding interface, and toxicity of ILs and their degradation by-products. Corrosion has been correlated to the chemical compositions of either the cation or the anion. For instance, Bermudez and Jimenez [49] reported that the chain length of the cation substituent influences corrosion. For ILs with the 1-alkyl-3-methylimidazolium cation, the

presence of short alkyl groups increases surface polarity, which in turn increases the wear and corrosion susceptibility of the aluminum and steel surfaces that they investigated. The chemical composition of the anion has also been experimentally observed to influence the propensity of the IL toward detrimental chemical reactions. Corrosion was found to be prevalent on metal substrates coated with fluorine-rich ILs, e.g., ILs where the anion is tetrafluoroborate or hexafluorophosphate. In this case, the anion is moisture-sensitive and may hydrolyze to generate hydrofluoric acid [32, 50]. To date, two approaches have been demonstrated to reduce corrosion. One way is through the selection of anions that are more hydrophobic in order to reduce hydrolysis. Caporali et al. [51] investigated an IL with the relatively more hydrophobic *bis*(trifluoromethanesulfonyl) amide anion coated on AZ91D magnesium alloy, where they found that the corrosion rate of Mg is negligible at room temperature. However, as shown in Fig. 2, this protection from corrosion is limited, as they observed that the corrosion rate (in the form of crevice corrosion) is appreciable at elevated temperatures (200 °C). The second corrosion reduction strategy is the incorporation of anti-corrosion additives such as benzotriazole (BTA), which has been demonstrated by both Liu et al. [52] and Yu et al. [53] as a viable method in preventing metal surface corrosion. In both cases, corrosion reduction was attributed to the formation of surface protective films such as $Cu_2O$, [Cu(–$C_6H_5N_3$)], $FeF_2$, $FeF_3$, $Fe_3O_4$, and $FePO_4$. Scanning electron micrographs showing the corrosion protection as a function of the added BTA is shown in Fig. 3.

The oxidation of ILs with the imidazolium cation and *bis*(trifluoromethanesulfonyl) amide anion has been reported by Minami et al. [54]. Subjecting the ILs to heating at 200 °C in air for 1000 h led either to the formation of solid deposits or the transformation of the IL into a dark liquid, both of which indicating advanced

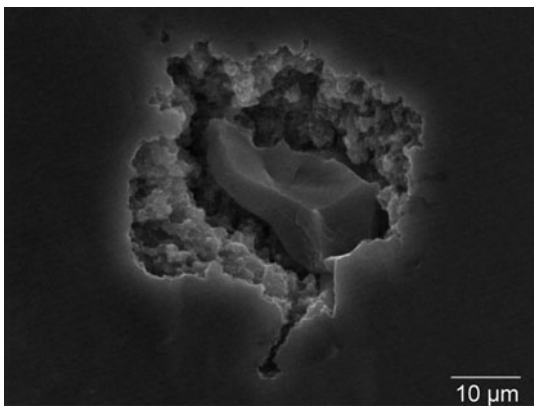


**Fig. 2** Crevice corrosion on the surface of AZ91D magnesium alloy immersed in 1-butyl-3-methylimidazolium *bis*(trimethylsulfonyl) imide at 200 °C for 30 days [51]

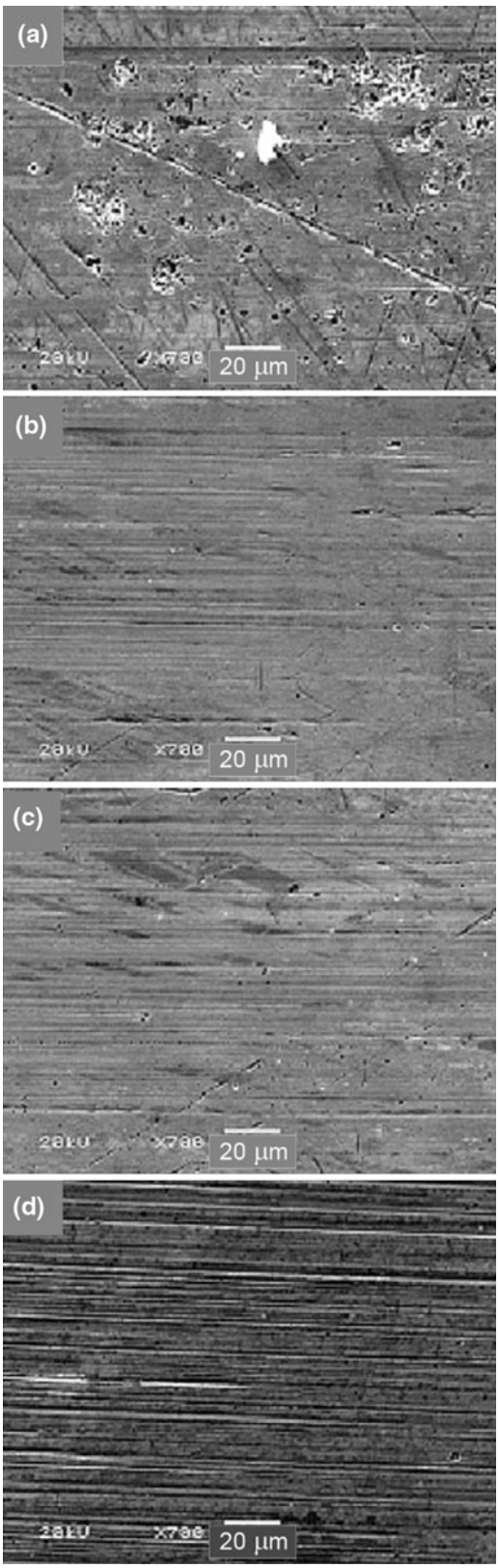


**Fig. 3** Scanning electron micrographs of worn bronze surfaces lubricated with 1-ethyl-3-hexylimidazolium hexafluorophosphate with BTA as additive. Images from *top to bottom* represent increasing amounts of added BTA: **a** no BTA added, **b** 0.05%, **c** 0.5%, and **d** 2% [52]

thermal oxidation. This was mainly attributed to the scission of the C–N bond due to the decomposition of the imidazolium cation [31, 54].

The occurrence of tribochemical reactions on IL-coated steel surfaces during tribotesting has been observed through surface analysis techniques such as X-ray Photoelectron Spectroscopy (XPS), Time-of-flight Secondary Ion Mass Spectroscopy (TOF-SIMS), and Mössbauer spectroscopy [22, 23, 31, 40, 55–57]. Tribochemical reactions in the presence of ILs resulted in the formation of protective films (such as $FeF_2$, $FeF_3$, $FePO_4$, FeS, and $B_2O_3$) on the worn steel surface, which is mostly regarded as beneficial due to the observed lowering of the coefficient of friction and improved wear resistance. An example of XPS spectra demonstrating the formation of protective films is shown in Fig. 4 [22]. Figure 4a is the Boron 1s spectra of neat 1-methyl-3-hexylimidazolium tetrafluoroborate on Au. Figure 4b and c are spectra of wear scars in the sliding area of sialon against steel and sialon against $Si_3N_4$, respectively, both lubricated with 1-methyl-3-hexylimidazolium tetrafluoroborate. The protective film BN was observed on sialon/steel, while $B_2O_3$ and BN were detected on the sialon/$Si_3N_4$ surfaces. However, the formation of a surface film may have an adverse effect as well. In the case of 1-ethyl-3-methylimidazolium tetrafluoroborate on steel, Philips et al. [57] reported that the formation of $FeF_2$ on the surface led to degradation of the IL and visual confirmation of corrosion. This is attributed to the $FeF_2$ acting as a Lewis acid site that can act as a catalyst of lubricant degradation, which in turn, leads to substrate corrosion.

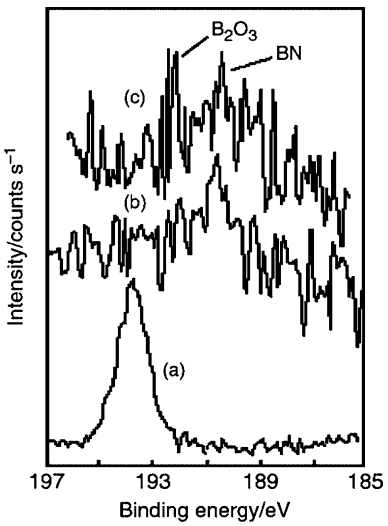


**Fig. 4** Boron 1s XPS spectra showing **a** neat 1-methyl-3-hexylimidazolium tetrafluoroborate on Au, **b** sliding of sialon against steel lubricated with 1-methyl-3-hexylimidazolium tetrafluoroborate leads to the formation of BN protective film, and **c** sliding of sialon against $Si_3N_4$ lubricated with 1-methyl-3-hexylimidazolium tetrafluoroborate leads to the formation of $B_2O_3$ and BN films [22]

Potential toxicity of ILs could arise due to its decomposition. Swatloski et al. [58] challenged the perceived "greenness" of ILs by pointing out that ILs containing the hexafluorophosphate anion can hydrolyze in contact with moisture. This results in the release of toxic volatile compounds such as HF and $POF_3$, which are known to damage materials such as steel and glass. This has led to the development of anions such as octylsulfate ($C_8H_{17}SO_4^-$), which aside from being halogen-free, is resistant to hydrolysis up to 80 °C [30, 59]. Cations have also been identified as potentially toxic. It was reported that ILs containing the imidazolium cation have toxicity levels comparable to common manufacturing chemicals such as ammonia and phenol [60]. This is a concern since as shown in Fig. 1a, the imidazolium cation is a typical component of ILs. Therefore, these observations on reactivity and toxicity should be considered in the selection of an IL lubricant for a given application.

Having discussed the issues that may affect the suitability of ILs as lubricants, emerging efforts on combining ILs with other materials should be noted. Carbon nanotubes (CNT), both single-walled and multi-walled types, have been pursued as an IL additive, and an improvement in the tribological properties was reported [61, 62]. Another route is by combining ILs with conventional oils. Through synthetic techniques, ILs can be attached to conventional lubricants such as phosphazenes and PFPEs [32, 48, 63]. Omotowa et al. [48] reported the synthesis of phosphazene/IL hybrids, where organic groups containing the ammonium or pyridinium cations were attached to the phosphazene ring, leading to multivalent cations (5–8 cations on each molecule). These novel molecules, which are designed as additives, enhance the solubility of ILs in conventional (nonpolar) lubricants, as well as improve the miscibility of organic oils in aqueous environments.

## 3 Lubrication Using ILs

We now review selected tribological and electrical studies on monocationic and dicationic ILs, and discuss proposed chemical bonding mechanisms that account for the lubricating properties of ILs. Initial tribological studies on ILs were mainly conventional tribology testing (ball-on-disk, four-ball configuration, etc.) of various material pairs commonly used in machinery, e.g., steel/steel, steel/Al, steel/$SiO_2$, steel/sialon, sialon/$Si_3N_4$, and the like [22–24, 44, 55]. Figure 5 is an example of ball-on-disk test results for steel/steel contact showing that the ILs used, namely, 1-ethyl-3-hexylimidazolium-*bis*(trifluoromethylsulfonyl)-imide and 1-ethyl-3-hexylimidazolium tetrafluoroborate (abbreviated as L-F206 and L-B206, respectively, in Fig. 5) had comparable coefficient of friction, but superior wear

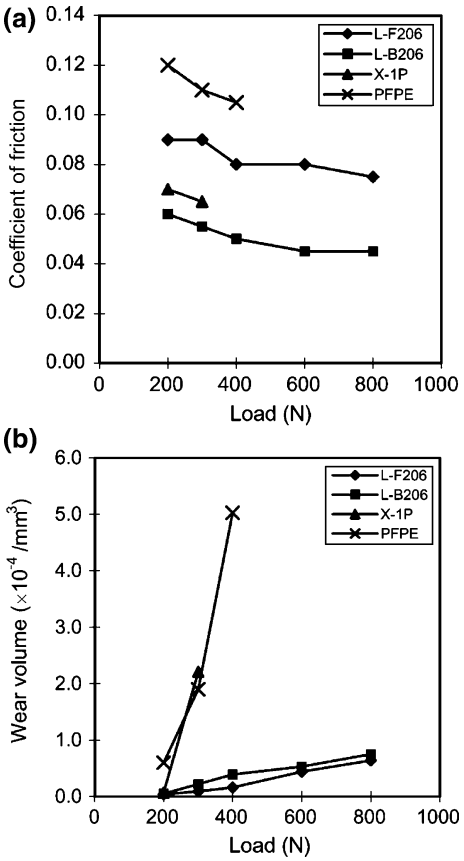


**Fig. 5** **a** Coefficient of friction and **b** wear volume of steel/steel contacts lubricated with the ILs 1-ethyl-3-hexylimidazolium-*bis*(trifluoromethylsulfonyl)-imide and 1-ethyl-3-hexylimidazolium tetrafluoroborate (abbreviated as L-F206 and L-B206, respectively) compared with the conventional lubricants X-1P and an unidentified PFPE lubricant at 20 °C [55]

resistance compared to the conventional lubricants X-1P (a phosphazene type lubricant) and an unidentified PFPE [55]. Ball-on-disk studies have also been made on various ILs coated on various silicon surfaces, such as surface-modified silicon (hydroxyl and amino-terminated surfaces), polysilicon, $SiO_2$, and $Si_3N_4$, where it was found that longer alkyl chains in the cation and the hydrophobic anions exhibit desirable tribological properties [64, 65]. Bermudez and coworkers reported pin-on-disk results on the application of ILs as lubricants for various polymers and polymer composites, such as those based on polystyrene, polycarbonate, and polyamides [46, 47]. As a result of these investigations, a good understanding exists on the macroscale tribological behavior of ILs on a wide range of materials.

Modeling studies have also been conducted in an effort to understand the interactions between ILs and the substrate where it is applied. In Fig. 6, an example of semi-empirical modeling of the interactions between a hydroxylated silicon surface and the IL 1-methyl-3-hydroxypropylimidazolium chloride is presented [66]. In this particular case, the cation contains a $–CH_2OH$ group as a substituent in the

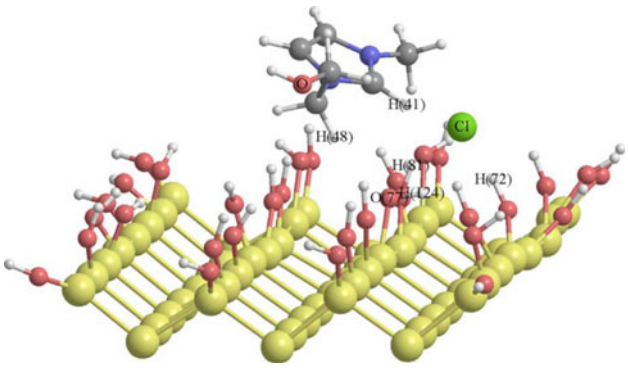


**Fig. 6** Semi-empirical modeling of interactions between a hydroxylated silicon surface and the IL 1-methyl-3-hydroxypropylimidazolium chloride, $C_7H_{13}N_2OCl$ [66]

imidazolium ring, which forms a complex with the silicon surface. Changing the nature of the side groups has an effect on the thermodynamic properties, as well as the calculated coefficient of friction. The calculated enthalpy of complex formation became more negative (indicating increased bonding between the silicon and the IL) and the coefficient of friction decreased as the substituent was varied in the following order:$–CH_2OH > –CN > –CH_3 > –COOH$ [66].

Experimental and modeling studies on IL films trapped (confined) between two surfaces provide a glimpse of their morphology, viscosity, and shear properties, which has implications on their use as nanodevice lubricants. From surface force apparatus (SFA) studies, Perkin et al. [67] measured shear forces and concluded that the irregular structure of the ions is responsible for the observed low shear stresses in ILs compared to organic liquids and hydrocarbon lubricants. Relative to bulk viscosity values, Ueno et al. [68] reported a 1–3 order of magnitude increase in the viscosity of ILs during confinement as measured by the SFA. Since ILs are electrically conductive, the viscosity response of confined ILs under an applied external electric field is also of interest. Xie et al. [69] observed that the viscosity of IL films increases with increasing strength of the applied electric field. This is attributed to the alignment of the cation side chains in the direction of the electric field. In modeling studies, molecular dynamics (MD) simulations have shown that IL films confined between rigid planar surfaces are capable of forming mesoscopic structures (or mesophases) composed of cation/anion clusters and of neutral regions formed by the cation side groups [70]. The formation of mesophases for may affect the viscosity and account for the tribological properties of confined ultrathin IL films. In another MD simulation study, Mazyar et al. [71] investigated the effect of ILs on the adhesion and friction of self-assembled monolayers (SAM) on $SiO_2$, where they found that the IL can possibly replace an area of the SAM damaged during sliding, thus improving the tribological properties.

Bhushan et al. [27] evaluated the commonly available IL 1-butyl-3-methyl-imidazolium hexafluorophosphate (abbreviated as BMIM-$PF_6$, Merck, Germany) deposited on Si(100) wafers using AFM techniques, which was found to exhibit improved friction and wear properties compared to conventional lubricants. A summary of the properties of BMIM-$PF_6$ relative to the conventional PFPE lubricant Z-TETRAOL, typically used in magnetic hard disk drives [1], is presented in Table 2. Both BMIM-$PF_6$ and Z-TETRAOL films were evaluated as untreated, partially bonded (by heating at 150 °C for 30 min after dip coating), and fully bonded (thermal treated and washed). The effect of thermal treatment is of interest because it influences the amount of mobile and immobile lubricant molecules, which in turn affects the ability of the lubricant film to form a meniscus. The tendency toward meniscus formation leads to stiction and influences the degree of bonding with the substrate, affecting durability.

The durability of IL films on various metal and ceramic substrates has been investigated from the standpoint of film formation (wettability) and film removal (friction and wear), where it was found that certain cations and anions cause ILs to exhibit improved wetting, friction reduction, and wear resistance properties [27]. In general, ILs exhibit better wettability on noble metal and ceramic surfaces than on non-noble metal surfaces [34]. The flat imidazolium cation shows poorer wettability compared to bulkier cations such as ammonium and sulfonium. Among salts with the imidazolium cation, the presence of longer organic side chains lead to a reduction of the coefficient of friction. An anion effect is also observed, where oxygen-rich anions show better substrate wettability and lower wear compared to other imidazolium salts.

The electrical properties of lubricated films are of interest because during sliding, charge buildup may occur on the surface, which could have an adverse effect on micro/nanodevices performance. The AFM can be configured to measure the change in electrical properties, and has been used to examine the change in the surface potential and contact resistance after sliding experiments [27, 29]. Aside from determining the occurrence of either charge dissipation or buildup, the results of these experiments can also be used to examine the extent of wear damage on the surface after sliding.

Dicationic ILs are of interest for tribological studies because the presence of long organic chains in their cations may promote favorable interactions with the substrate as well as improved organization of the molecular chains. Some dicationic ILs are thermally stable up to 400 °C [72]. The adhesion and friction properties of two dicationic IL films on Si(100) substrate, based on the imidazolium cation and the *bis*(trifluoromethanesulfonyl) amide (or "triflamide") anion, were studied by Palacio and Bhushan [29] and their properties were compared to the conventional monocationic IL BMIM-$PF_6$. The dicationic ILs used were 1,1′-(pentane-1,5-diyl)*bis* (3-hydroxyethyl-1*H*-imidazolium-1-yl) di[*bis*(trifluoromethanesulfonyl) amide)] (abbreviated as BHPT) and 1, 1′-(3,6,9,12,15-pentaoxapentadecane-1,15-diyl)*bis*(3-hydroxyethyl-1*H*-imidazolium-1-yl) di[*bis*(trifluoromethanesulfonyl) amide)] (abbreviated as BHPET) [73]. Their chemical structures are shown in Fig. 7. These compounds have been applied on single-crystal Si(100) (phosphorus doped) with a native oxide layer on the surface using the dip coating technique. The films were heat-treated at 150 °C for 30 min after dip coating, such that they were partially bonded [27].

Atomic force microscopy experiments were also performed by Palacio and Bhushan [29] at various humidity and temperature conditions in order to investigate the effect of the environment on the nanolubrication properties of these ILs. Macroscale friction and wear experiments using the ball-on-flat tribometer and wear at ultralow loads using an AFM were carried out. Fourier Transform Infrared (FTIR) spectroscopy and XPS were used to determine the chemical species that affect intermolecular bonding and also to elucidate the effect of the environment on the IL film surface in the case of FTIR data.

A review of the work on the tribological properties of monocationic and dicationic ILs using the AFM follows.

## 3.1 Monocationic IL properties

In this section, nanotribological data on BMIM-$PF_6$ and Z-TETRAOL (for comparison) are presented [27–29].

### *3.1.1 Nanotribological Studies*

Bhushan et al. [27] compared the nanotribological properties of BMIM-$PF_6$ to a conventional PFPE, Z-TETRAOL.

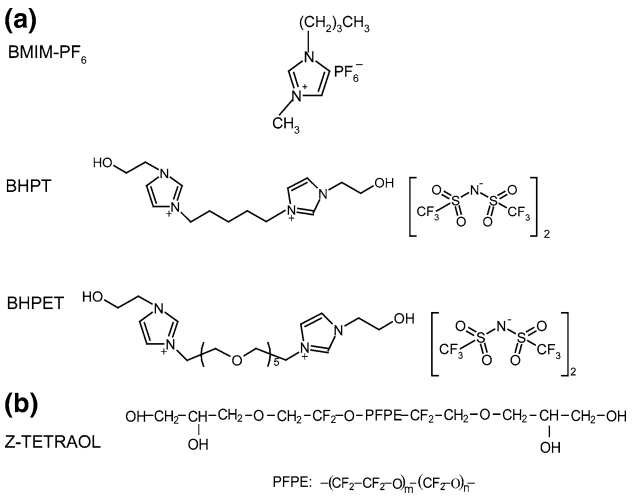


**Fig. 7** **a** Chemical structures of the BMIM-$PF_6$, BHPT, and BHPET molecules and **b** chemical structure of the Z-TETRAOL molecule (adapted from [29])

Figure 8a is a summary of the adhesive force and coefficient of friction measurements on the IL, relative to Z-TETRAOL and Si(100). The adhesive force was observed to decrease in the following order: untreated > partially bonded > fully bonded. This mobile fraction on the untreated sample facilitates the formation of a meniscus, which increases the tip–sample adhesion. The adhesive force is highest in the untreated coating since it has the greatest amount of the mobile fraction among the three samples. Conversely, the sample with no mobile lubricant fraction available (fully bonded) has the lowest adhesive force.

A different trend is observed in the coefficient of friction ($\mu$) data. Both the fully bonded and partially bonded samples have lower $\mu$ values compared to the uncoated silicon. Friction forces are lower on the latter, implying that the mobile lubricant fraction present in the partially bonded samples facilitates sliding of the tip on the surface. However, $\mu$ values for the untreated samples are higher than the data for the heat-treated coatings. Due to the lack of chemical bonding, the interaction of the lubricant to the substrate is weakened and dewetting can occur. Water and lubricant molecules are more likely to form a meniscus as the tip approaches the surface. This provides greater resistance to tip sliding, leading to higher coefficient of friction values. It is worth noting that comparable results were obtained by other groups who performed AFM-based adhesion and friction measurements on untreated IL films on silicon [74–78]. The role of meniscus formation in the adhesive and friction forces obtained for the uncoated Si and the untreated, partially bonded and fully bonded lubricant-coated Si surfaces is depicted in the schematic at the lower portion of Fig. 8a [27].

Figure 8b contains plots of the coefficient of friction as a function of the number of sliding cycles at 70 nN normal load. Only a small rise in the coefficient of friction was observed for both Z-TETRAOL and the BMIM-$PF_6$ surfaces, indicating low surface wear. In the case of untreated Z-TETRAOL, a crossover is observed, where the coefficient of friction increases from its initial value and exceeds the $\mu$ of silicon after a certain number of cycles. This is attributed to the transfer of lubricant molecules to the AFM tip and the interaction of the transferred molecules with the lubricant still attached on the Si substrate, which will increase the friction force.

### 3.1.2 Nanoscale Electrical Studies

Since the measurement of electrical properties such as surface potential and resistance can be used to monitor charge buildup as well as the extent of the wear region on the surface, the study by Bhushan et al. [27], where AFM-based electrical properties mapping in conjunction with nanoscale wear tests was conducted, is now reviewed. In this study, a diamond tip was used to create 5 × 5 $\mu m^2$

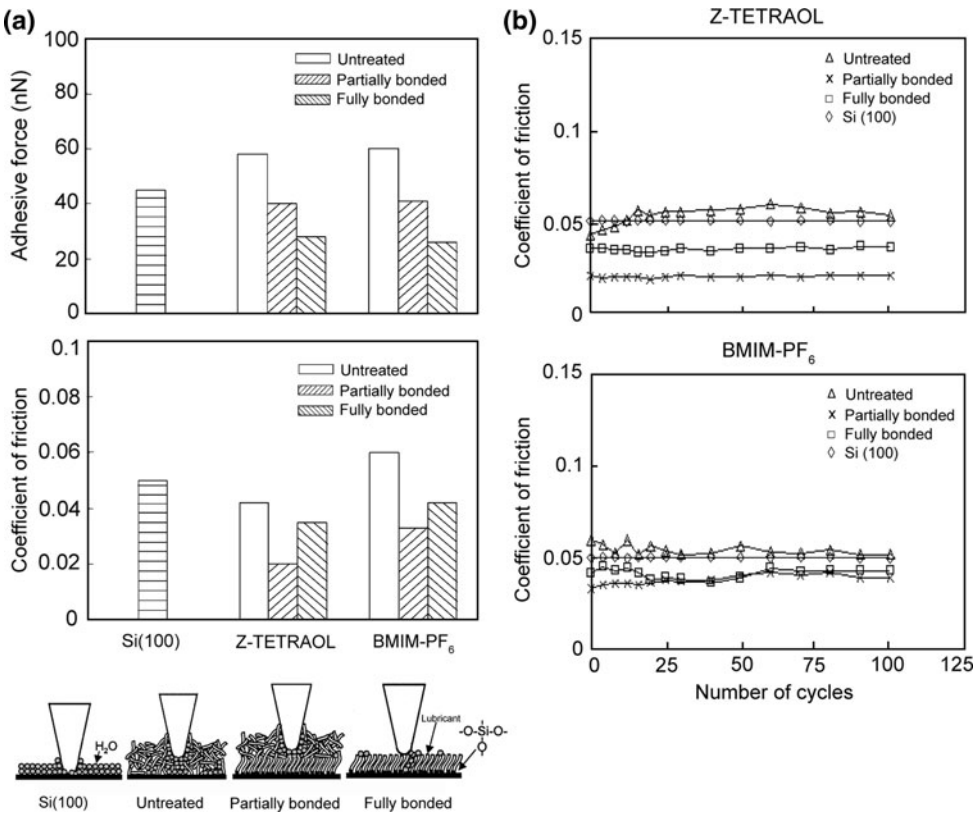


**Fig. 8** **a** Summary of the adhesive force and coefficient of friction and **b** durability data after 100 cycles for BMIM-$PF_6$ at room temperature (22 °C) and ambient air (45–55% RH). Data for the uncoated Si and Z-TETRAOL are shown for comparison. Schematic in **a** shows the effect of chemical bonding treatment and meniscus formation between the AFM tip and sample surface on the adhesive and friction forces [27]

wear scars at a load of 10 μN. Figure 9a is a bar plot summarizing the average surface potential change on the tested area of the IL- and PFPE-coated surfaces, relative to unlubricated Si surface. In general, the samples containing the mobile lubricant fraction (i.e., untreated and partially bonded surfaces) exhibit a lower surface potential change compared to the fully bonded sample, which only has immobile lubricant molecules. This is attributed to lubricant replenishment by the mobile fractions, which can occur in the untreated and partially bonded samples [79]. From Fig. 9a, it is also observed that the change in surface potential is generally lower in the IL coatings compared to the Z-TETRAOL coatings and the uncoated silicon. This indicates that any built-up surface charges arising from the wear test were immediately dissipated onto the conducting ionic lubricant coating surface. In the case of Z-TETRAOL and the uncoated silicon, the charges remained trapped in the test area, since both these materials are insulators. Based on these findings and previous observations [79–81], a considerable surface potential change will be observed on the wear region when: (1) the lubricant has been fully removed from the substrate; (2) the native $SiO_2$ layer has been abraded from the surface; (3) wear has caused subsurface structural changes; and (4) charges build up as they are unable to dissipate into the surrounding material.

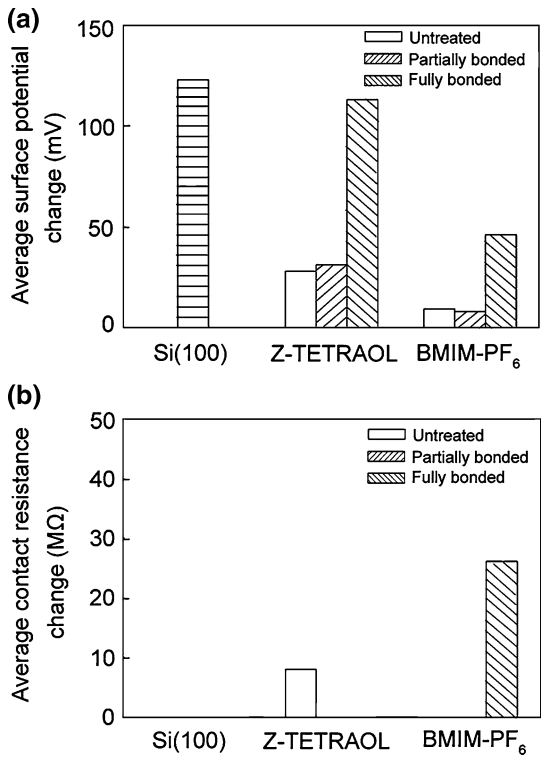


**Fig. 9** **a** *Bar chart* showing average surface potential change for various BMIM-$PF_6$ coatings and **b** *bar chart* showing average contact resistance change for various BMIM-$PF_6$ coatings. In both cases, data for Z-TETRAOL and uncoated Si are shown for comparison [27]

The average change in the contact resistance of the wear region relative to the untested area is summarized in Fig. 9b. The fully bonded BMIM-$PF_6$ has appreciable contact resistance increase in the wear region. Since silicon is a semiconductor, it has much higher resistance compared to the surrounding IL. The resistance increase in the worn area implies that the substrate is exposed after the wear test. Partially bonded films did not get worn out from the substrate after the test, as evidenced by the lack of contact resistance change in the tested area. The untreated Z-TETRAOL-coated surfaces exhibited an observable resistance change, while BMIM-$PF_6$ did not. This can be correlated to the durability data in Fig. 8b, where the untreated Z-TETRAOL sample exhibited an increase in the friction force with time due to transfer of lubricant molecules to the tip. Easier lubricant removal means that the diamond tip can cause substrate wear much sooner, leading to the observed resistance increase in the tested area. However, the resistance image does not provide a clear contrast between Z-TETRAOL and the newly exposed substrate since both materials have high resistance values.

### *3.1.3 Conventional Tribological and Electrical Studies*

In order to compare friction and wear properties on the nanoscale with that on the macroscale, conventional ball-on-flat tribometer experiments were conducted on the same samples [27]. Images and profile traces of the wear scars are shown in Fig. 10a. The coefficient of friction and number of cycles to failure are summarized in Fig. 10b. The partially bonded BMIM-$PF_6$ shows comparable durability to its Z-TETRAOL counterpart. The nanoscale data presented in Fig. 8 can be compared to $\mu$ values obtained from ball-on-flat (Fig. 10b). The $\mu$ values of the untreated lubricant samples obtained by using AFM are lower than the $\mu$ obtained from the ball-on-flat tests. This is attributed to the difference in the length scales of the test techniques. An AFM tip simulates a single asperity contact while the conventional friction test involves the contact of multiple asperities present in the test system [3–5]. With regard to wear, the interface contact of the AFM and ball-on-flat techniques is different from each other. In an AFM, the contact stress is very high (since the contact area in AFM is much smaller compared to that of the ball-on-flat experiment) such that material can be displaced more easily. For a ball-on-flat test, the ball exerts a lower pressure on the surface, and the coating is in a confined geometry. As a consequence, displacement of the coating is not as easy as in AFM, leading to enhanced wear resistance.

Macroscale contact resistance obtained from ball-on-flat tribometer testing is shown in Fig. 11, along with the corresponding coefficient of friction data. For the IL film, the initial resistance is slightly lower than that of uncoated

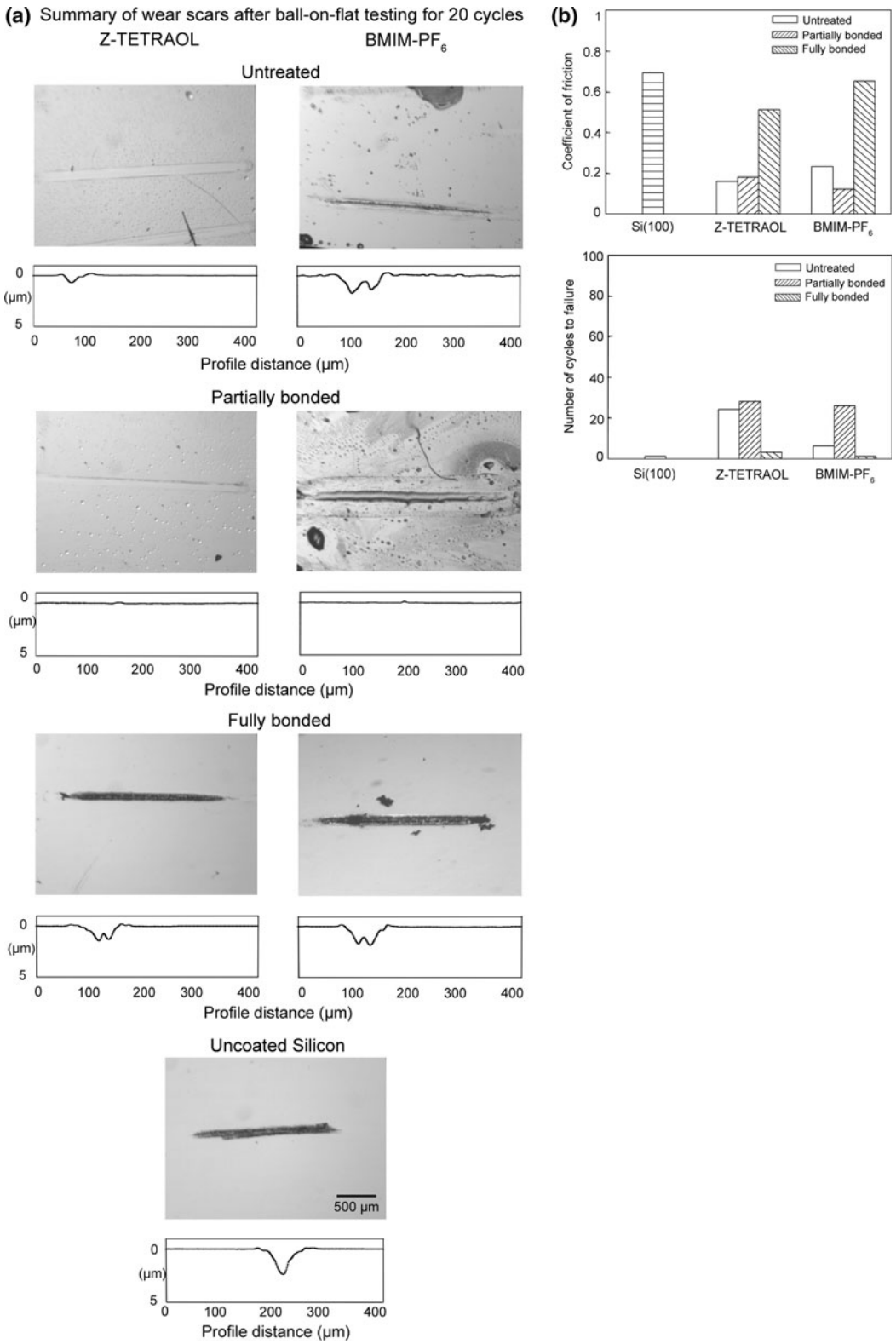


**Fig. 10** **a** Optical images and height profiles taken after 20 cycles and **b** summary of the coefficient of friction and number of cycles to failure from ball-on-flat tests on various BMIM-$PF_6$ coating. Data for the uncoated Si and Z-TETRAOL are shown for comparison [27]

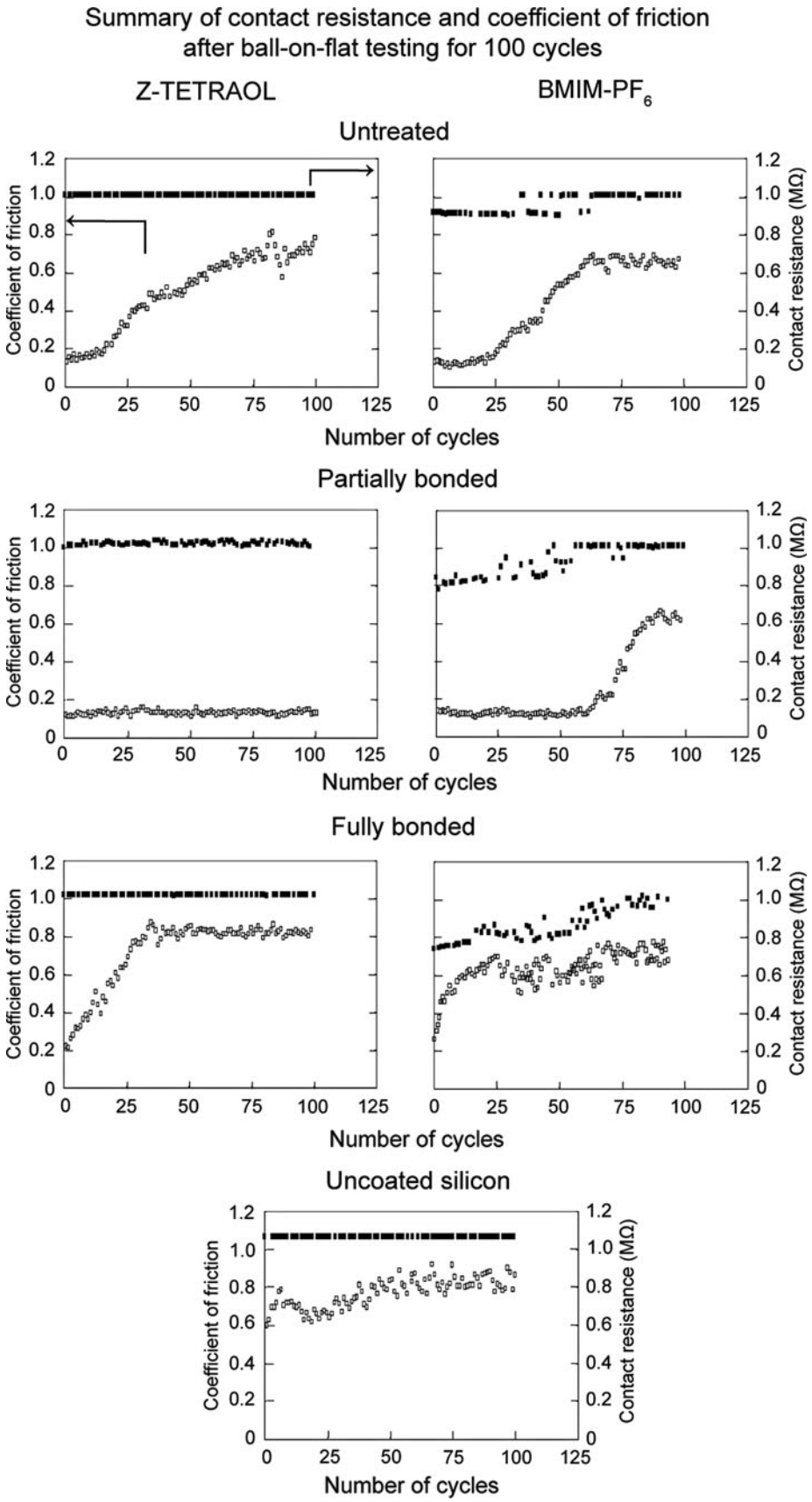


**Fig. 11** Contact resistance and coefficient of friction after ball-on-flat tests for 100 cycles on various BMIM-$PF_6$ coatings. Data for the uncoated Si and Z-TETRAOL are shown for comparison [27]

silicon, confirming their conductive nature. For the Z-TETRAOL samples, the contact resistance is about the same magnitude as the uncoated silicon. But for the conducting IL, an increase in resistance corresponds to an increase in the coefficient of friction, indicating wear of the lubricant and exposure of the silicon substrate, similar to observations in the nanoscale. These results are consistent with the adhesion, friction, and surface potential results with regard to wear detection and wear protection coming from the mobile and immobile lubricant fractions [27].

The durability data and trends for the IL obtained by using a steel ball shown in Fig. 11 are somewhat comparable to the trends in Fig. 10, which was measured by using a sapphire ball. In Fig. 11, the partially bonded samples still show the best durability, and in this case, the Z-TETRAOL films consistently took longer to fail compared to BMIM-$PF_6$, as indicated by the point where the jump in the coefficient of friction is observed. This can be accounted for from the wetting properties of ILs on different surfaces. It has been observed that ILs have a tendency to wet nonmetal surfaces (e.g., $Si_3N_4$, $SiO_2$, and glass) better than conventional metal surfaces (such as 440C, M50, and 52100 steel) [27]. Less wettability could lead to less lubricant retention at the interface. This material wetting effect is possibly more significant for the IL than in Z-TETRAOL, but nonetheless, the durability of the partially bonded BMIM-$PF_6$ is still close to its Z-TETRAOL counterpart, such that ILs are still viable lubricants comparable to PFPEs.

## 3.2 Dicationic IL Films

In this section, nanotribological data on BHPT and BHPET are presented. Data on BMIM-$PF_6$ and uncoated Si(100) are also presented for comparison [29].

### *3.2.1 Nanotribological Studies*

Palacio and Bhushan [29] investigated the nanotribological properties of dicationic liquids relative to a monocationic liquid and uncoated Si through AFM studies. Figure 12a is a summary of the contact angle (with deionized water), adhesive force, and coefficient of friction ($\mu$) measurements for the coated and uncoated samples performed at ambient temperature and humidity conditions (22 °C and 50% RH, respectively). The data shown in the bar plots are the averages of three measurements and the error bars represent $\pm 1\sigma$. BHPT is the least hydrophilic as it has the highest contact angle (81°) among the three IL coatings. For comparison, the water contact angles of BMIM-$PF_6$ and BHPET are 39 and 59°, respectively. The BHPT coating also exhibited the greatest reduction in the coefficient of friction relative to the uncoated surface. The high

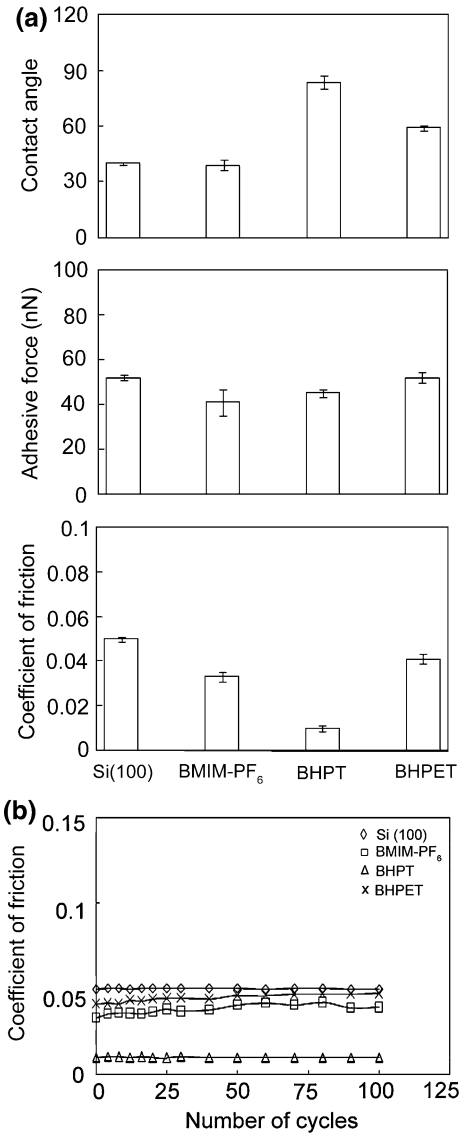


**Fig. 12** **a** Summary of the contact angle, adhesive force and coefficient of friction and **b** durability data after 100 cycles for BMIM-$PF_6$, BHPT and BHPET coatings at room temperature (22 °C) and ambient air (45–55% RH). Data for uncoated Si are shown for comparison. The *error bars* in **a** represent $\pm 1\sigma$ based on three measurements performed [29]

contact angle of BHPT leads to minimal meniscus formation between the tip and surface, leading to a large drop in the nanoscale friction force. In addition, BHPT has a pentyl chain which links the two imidazolium cations. This chain can orient the cation molecules on the substrate, thereby facilitating tip sliding on the film surface. In contrast, the polyether chain of BHPET is susceptible to interactions with water molecules which can promote (instead of minimize) meniscus formation. The BMIM-$PF_6$ film also exhibited a reduction in the adhesive force and coefficient of friction. This comes from the combination of mobile and immobile lubricant fractions. Immobilization of this IL is

possible as a result of the thermal treatment, which promotes the reaction between the hexafluorophosphate anion with the hydroxyl groups present on the silicon substrate surface [27, 29, 82].

Wear tests were conducted using an AFM by Palacio and Bhushan [29] by monitoring the change in the friction force on a 2-μm line for 100 cycles. Figure 12b shows representative data focusing on the wear of the lubricant film on the substrate. The $\mu$ value of the BHPT film changed minimally during the duration of the experiment, which indicates that the film was not being worn after 100 cycles. On the other hand, the BMIM-$PF_6$ and BHPET samples exhibited a gradual increase in $\mu$, which means that these films could be undergoing some wear and that their interaction with the silicon substrate is weaker compared to that of BHPT.

The effect of the environment [relative humidity (RH) and temperature] on the nanotribological properties was studied by Palacio and Bhushan [29]. The influence of RH on adhesion and friction is summarized in Fig. 13. In general, the adhesive force increases with the RH. The condensed water in the humid environment facilitates meniscus formation between the tip and sample and higher adhesive forces. Since Si(100) is hydrophilic, it readily adsorbs water molecules. For the three ILs, an increase in the adhesive force is also due to increased water adsorption. This comes from attractive electrostatic interactions (ion–dipole forces) between the individual ions and water molecules.

Water adsorption affects the observed coefficient of friction as a function of the RH. In Si, the coefficient of friction is uniform at 10–50% RH, then decreases at 70% RH. The adsorbed water at higher humidity can lead to the formation of a continuous water layer separating the tip and sample surface, which can act as a lubricant. Although the adhesive force increases, the reduction in interfacial strength accounts for the slight decrease of the coefficient of friction at the highest range of humidity level examined. However, the presence of more water molecules at higher humidity has an opposite effect on the IL surfaces, where the coefficient of friction increases with humidity. The attractive ion–dipole forces between the ions and water are amplified at higher humidity because more water molecules are available. A greater attractive force between tip and surface leads to greater resistance to sliding and a higher coefficient of friction. This is observed on both the monocationic (BMIM-$PF_6$) and the dicationic (BHPT and BHPET) IL-coated surfaces. For BHPET, polar interactions between water and the oxygen atoms in the polyether (C–O–C) chain is possible and increases the water adsorption to the surface. This could account for the larger rise in the coefficient of friction in the BHPET sample from 50 to 70% RH, compared to BMIM-$PF_6$ and BHPT [29].

The effect of temperature on the adhesion and friction properties of the ILs is summarized in Fig. 14. The adhesive and friction forces were measured from 22 to 125 °C. As shown in Fig. 14, the increase in test temperature leads to a decrease in the adhesive force and the coefficient of friction. The decrease in the adhesive force at higher temperatures is observed in all the samples, while the corresponding drop in the coefficient of friction is seen only for BMIM-$PF_6$, BHPET, and the silicon substrate. At higher temperatures, the surface water molecules are

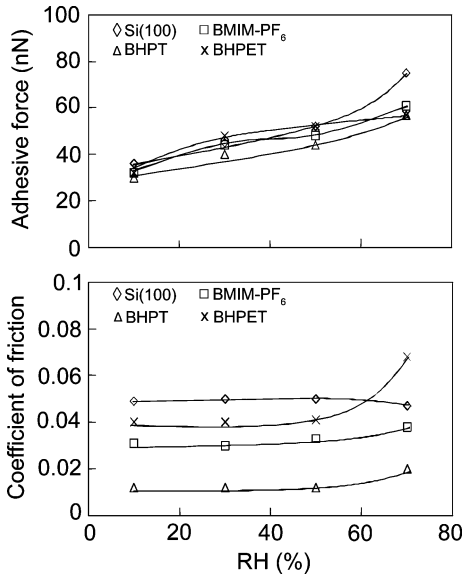


**Fig. 13** Influence of the RH on the adhesive force and coefficient of friction for unlubricated and lubricated tapes at 22 °C [29]

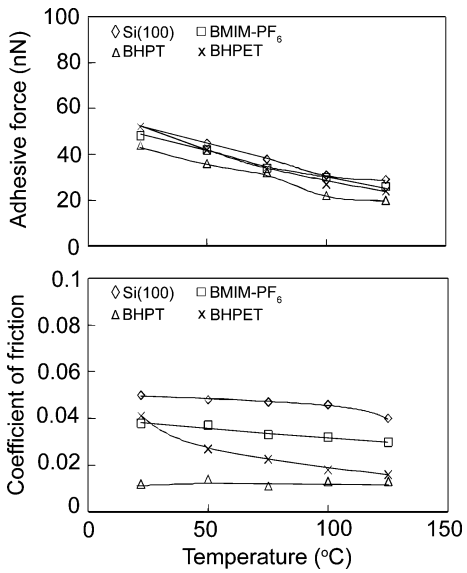


**Fig. 14** Influence of temperature on the adhesive force and coefficient of friction for uncoated and coated Si samples at 50% RH air [29]

desorbed, leading to the decrease in both the adhesive and friction forces. A reduction in the viscosity at higher temperatures can also facilitate the decrease in the friction force [13]. In BHPT, the coefficient of friction was not adversely affected as the test temperature was increased. This implies that at ambient humidity conditions, the BHPT film does not adsorb a large amount of water molecules. Moreover, this also implies that the BHPT surface has weak interactions with surface water molecules, such that friction force during sliding is not very much affected [29].

### 3.2.2 Nanoscale Electrical Properties

Figure 15 is a summary of the average contact potential change after the wear tests conducted by creating $5 \times 5$ $\mu m^2$ wear scars with a diamond tip, where the height and surface potential maps were imaged afterward. A change in the surface potential in the wear region is observed when the following occur: the lubricant has been fully removed from the substrate, the native $SiO_2$ layer has been abraded from the surface, wear has caused subsurface structural changes, and charges build up as they are unable to dissipate into the surrounding material [27, 29]. As expected, the uncoated Si exhibited the greatest amount of wear (as evidenced by debris buildup around the edge of the wear test region) and highest increase in the surface potential. The surface potential image for BHPET film also showed an increase, indicating that the film was worn out after the test. This was not seen on tests with the BMIM-$PF_6$ and BHPT samples. The surface potential change could be absent in the test area if the lubricant was not removed completely, indicating that these two samples have a stronger interaction with the silicon substrate compared to BHPET.

Figure 16 shows a summary of the average contact resistance change after the wear test. As shown in Fig. 15, a significant change is observed in the wear region of the Si and BHPET samples. There is also a small amount of localized contact resistance increase in the BMIM-$PF_6$ sample. These results are consistent with the cycling test presented in Fig. 12b, where the films are in this order of decreasing durability: BHPT > BMIM-$PF_6$ > BHPET.

### 3.2.3 Conventional Tribological Studies

In order to compare friction and wear properties at the macroscale and the nanoscale, conventional ball-on-flat tribometer experiments were conducted by Palacio and Bhushan [29] on the same samples. The average coefficient of friction data are summarized in Fig. 17. All of the lubricated samples are reported to have less wear scars as a

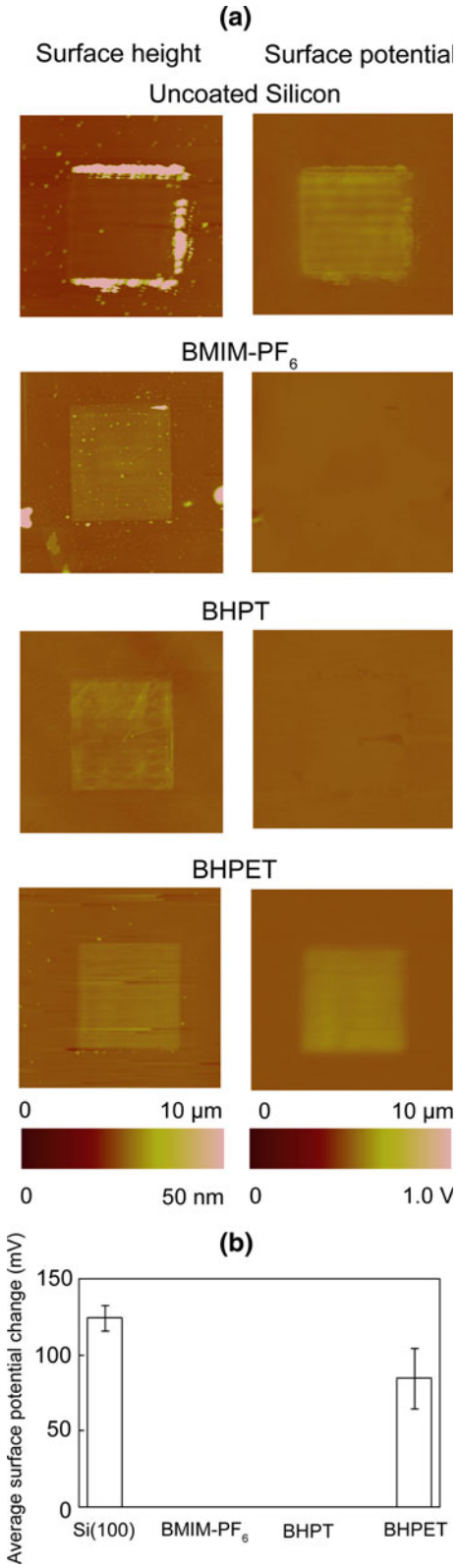


**Fig. 15** **a** Surface height and surface potential maps after wear tests and **b** *bar chart* showing average surface potential change for BMIM-$PF_6$, BHPT, and BHPET coatings. Data for uncoated Si are shown for comparison. The *error bars* represent $\pm 1\sigma$ based on three measurements performed [29]

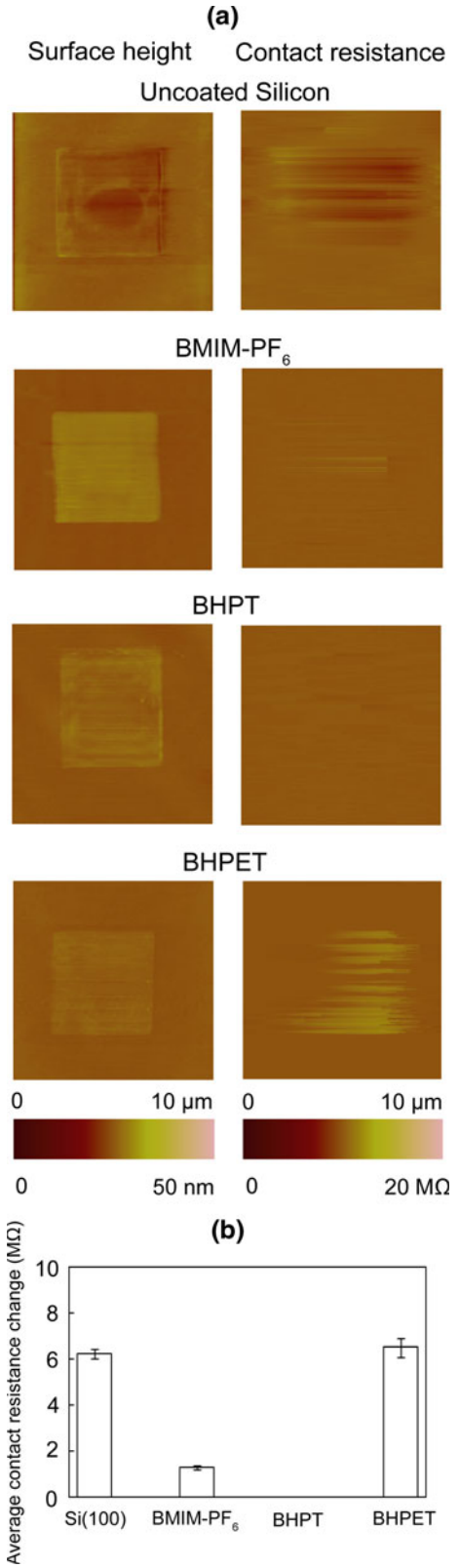


**Fig. 16** **a** Surface height and contact resistance maps after wear tests and **b** *bar chart* showing average contact resistance change for BMIM-$PF_6$, BHPT, and BHPET coatings. Data for uncoated Si are shown for comparison. The *error bars* represent $\pm 1\sigma$ based on three measurements performed [29]

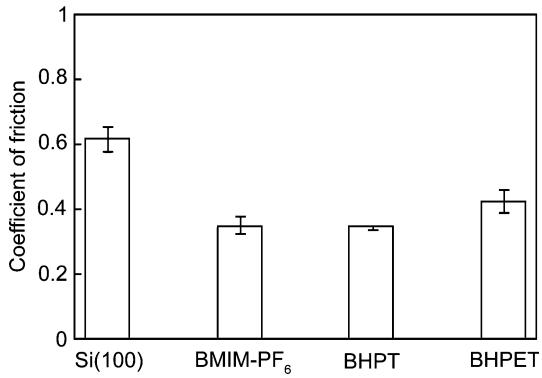


**Fig. 17** Summary of the coefficient of friction from ball-on-flat tests on uncoated and coated Si samples. The *error bars* represent $\pm 1\sigma$ based on three measurements performed [29]

result of the ball having to displace the lubricant before damaging the silicon surface. A reduction in the coefficient of friction arising from application of the lubricant film is observed, which are consistent with the nanoscale adhesion, friction and wear results.

The coefficient of friction values of the lubricant samples obtained by using AFM are lower than those obtained from the ball-on-flat tests. As indicated earlier, this is attributed to the difference in the length scales of the test techniques. An AFM tip simulates a single asperity contact while the conventional friction test involves the contact of multiple asperities present in the test system. With regard to wear, the interface contact of the AFM and ball-on-flat techniques is different from each other such that one cannot expect both tests to show the same trend. On an AFM, the tip stress is very high such that material can be displaced more easily. For a ball-on-flat test, the tip exerts a lower pressure on the surface, and the coating is in a confined geometry.

## 3.3 Spectroscopic Analysis and Proposed Mechanisms for IL Lubrication

### *3.3.1 FTIR Spectroscopy*

Figure 18 is a summary of the FTIR spectra obtained for the different IL-coated samples, along with the uncoated Si substrate [29]. The observed peaks are labeled with the chemical bonds which they correspond to. In the case of the Si substrate (with a contact angle of 40°) exposed to water molecules in the ambient, no peaks are observed. C–H stretching vibrations in the coated samples are observed at the 600–800 $cm^{-1}$ range. For BHPET, the strong peak at $\sim$1060 $cm^{-1}$ is for the C–O–C vibration, which is prominent due to the presence of the polyether chain in its cation. This peak overlaps with the C–O

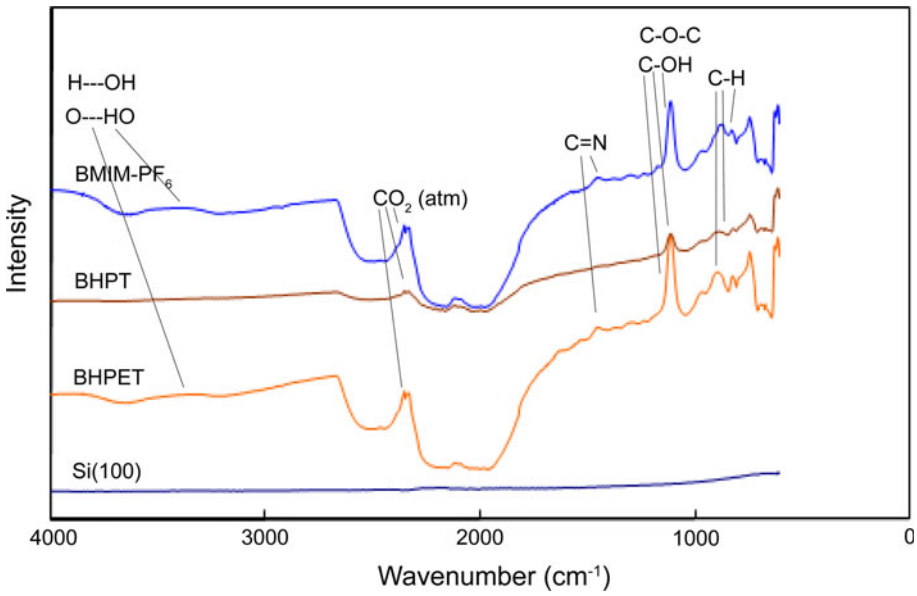


**Fig. 18** FTIR spectra of uncoated and coated Si samples. The chemical bonds (or species) were listed above the spectra to indicate the possible bonding modes that correspond to the observed peaks [29]

vibration, which is present in BHPT as the terminal primary alcohol (C–OH). In BMIM-$PF_6$, a peak appears in this range due to rocking vibrations of the methyl ($CH_3$) substituent. The peak at 1500–1600 $cm^{-1}$ comes from the C=N vibrations, which is common to all three ILs since they are all based on the imidazolium cation. However, it is not observed in BHPT as the C=N vibrations may be weak. The wide peak at 3600–4000 $cm^{-1}$ was attributed to hydrogen bonding, possibly due to water molecules adsorbed on the surface [29, 83]. This is present in BMIM-$PF_6$ and in BHPET but not in BHPT. This accounts for the much lower contact angle of BMIM-$PF_6$ and BHPET (39 and 59°, respectively) compared to BHPT (81°). This implies that the surface of BHPT is more hydrophobic compared to either BMIM-$PF_6$ or BHPET, which is consistent with the observed low coefficient of friction for BHPT [29].

### *3.3.2 XPS*

The XPS spectra for the uncoated Si samples have prominent peaks corresponding to Si and O, while the IL-coated samples contain peaks corresponding to Si, C, O, and F [29]. The high resolution, best-fit XPS spectra are shown in Fig. 19 for the Si 2p, C 1s, O 1s, and F 1s electrons. The peaks are labeled with the corresponding chemical bonds, which pertain to either the silicon substrate or groups found on the IL molecule. One noteworthy exception is the presence of peaks at approximately 292 eV, which confirms the presence of $CF_2$ on the surface. This indicates the immobilization of the BHPT and BHPET ILs, which occurs by the reaction of the anion with the hydroxyl groups present on the silicon surface [29].

### *3.3.3 Proposed Lubrication Mechanisms*

Figure 20 is an interpretation of how the IL cations interact with the silicon substrate [29]. For the monocationic BMIM-$PF_6$, only weak interactions between the imidazolium ring and the silicon surface are expected. This is similar to the proposed mechanism by Nainaparampil et al. [26], where the imidazolium cation was considered as mobile, while the anion is the species responsible for attachment to the silicon substrate.

However, for the dicationic ILs, multiple cation attachment schemes are possible. In BHPT, the hydroxyl groups attached to the imidazolium cation at the ends of the chain provide a means for strong H-bonding interactions with active sites on the silicon surface. As shown in Fig. 20, either one (case 1) or two (case 2) hydroxyl groups can create this bond. The second case is particularly desirable because if the two hydroxyl groups are bonded (i.e., not exposed to the surface), they are not available to interact with water molecules in the ambient, leading to a reduction in the adhesion and friction forces, as well as enhanced wear resistance [29].

In BHPET, these hydroxyl group attachment schemes are also applicable. However, the additional mechanism of intramolecular hydrogen bonding can also take place (case 3). This is not as desirable as the second case because it depletes the available chain ends with hydroxyl groups which can bond to the silicon surface. The interaction of the lubricant film with the silicon substrate is weakened, and water molecules can displace the lubricant from the substrate. In addition, the polyether chain that links the two cations contains five oxygen atoms in each chain. These oxygen atoms can also form H-bonds with

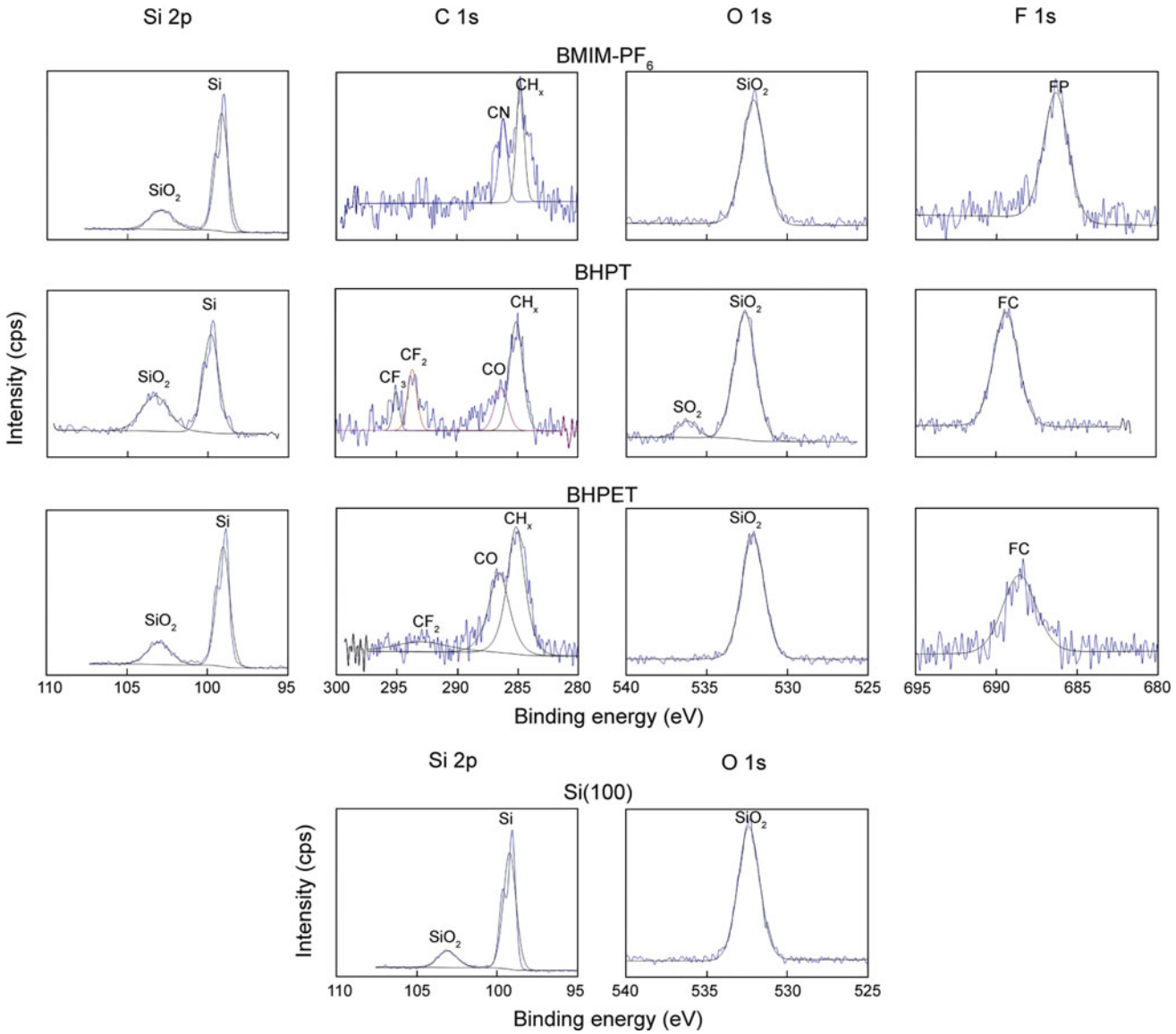


**Fig. 19** High-resolution (deconvoluted) XPS spectra for Si 2p, C 1s, O 1s and F 1s reveals the different binding environments present on the surface of uncoated and coated Si samples (adapted from [29])

the water molecules in the ambient. This can account for the large difference in the friction properties between BHPET and BHPT. While the application of the BHPT film has lowered the coefficient of friction of the silicon surface, the BHPET film did not have a similar effect due to the molecular interactions described above. This interpretation of lubricant–substrate interaction is corroborated by the adhesion and friction data at varying humidities and temperatures, as well as the FTIR spectra. Both BMIM-$PF_6$ and BHPET have large peaks in their FTIR spectra that correspond to H-bonds of water molecules, which is consistent with the observed sensitivity of their adhesion and friction to the change in humidity and temperature. Meanwhile, BHPT does not have the aforementioned peak, and its adhesion and friction properties appear to be less sensitive to water molecules compared to the other two ILs [29].

Figure 21 is a schematic showing the interaction of the anions with the silicon substrate. As mentioned previously, XPS spectra indicate immobilization of the IL, which occurs through the reaction of the anion with the hydroxyl groups on the substrate surface. In BMIM-$PF_6$, the O attaches to P, while in BHPT and BHPET (which have the same anion), the O bonds to C. Since the reactions involve the creation of new covalent bonds, this implies that the anions of the ILs investigated are more strongly attached to the substrate compared to the cations, which are chemically adsorbed [29].

Based on the macro- and nanoscale friction and wear measurements, the ILs show strong potential as lubricants

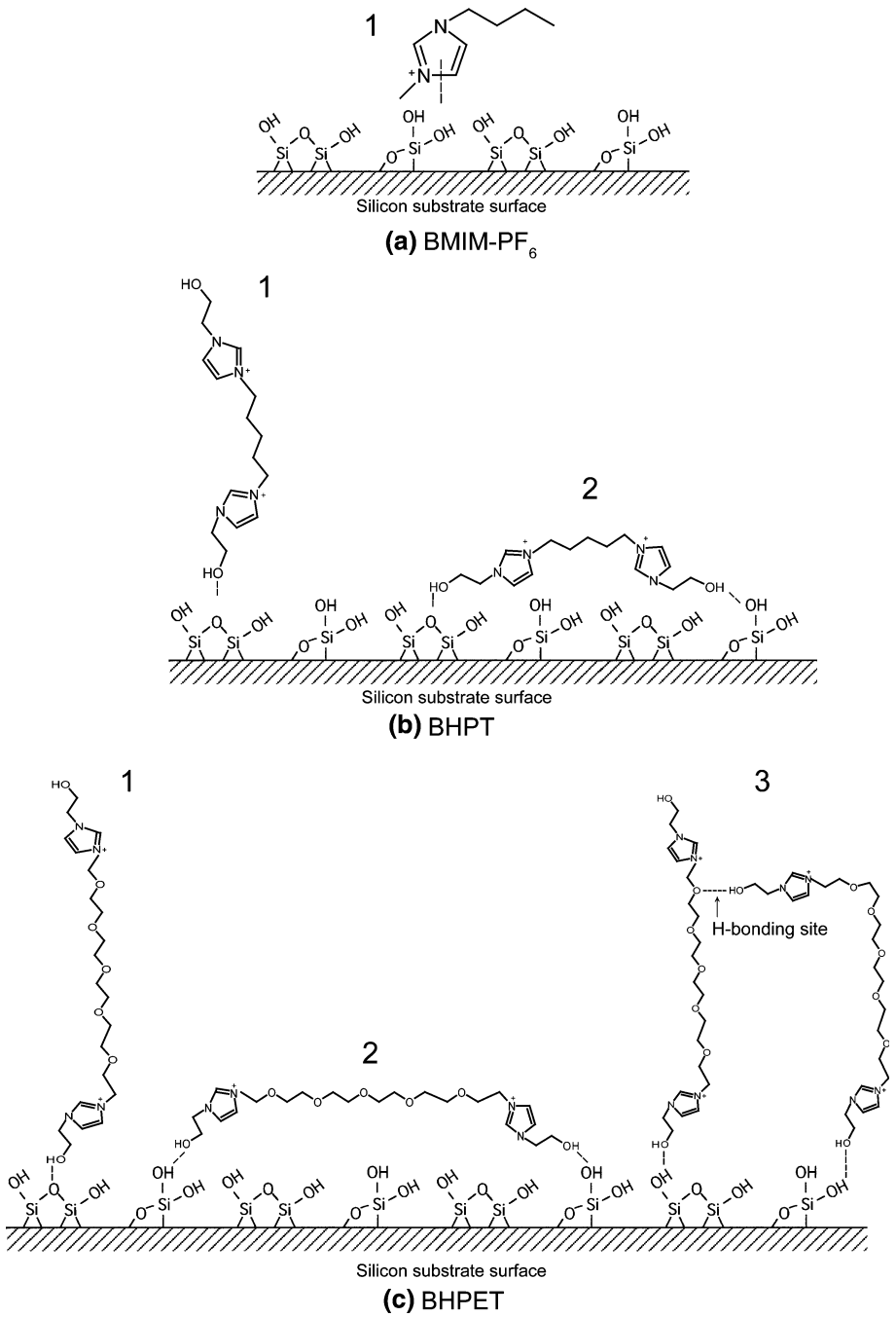


**Fig. 20** Schematic for the attachment of the cations of **a** BMIM-$PF_6$, **b** BHPT, and **c** BHPET to the silicon substrate [29]

for nanodevice applications. Aside from their inherent properties, such as their desirable thermal and electrical conductivity, and "greenness" (depending on the choice of IL), ILs exhibit desirable tribological properties, which are even superior to PFPEs in some instances.

## 4 Outlook

Ionic liquids are desired as lubricants due to their electrical conductivity, thermal conductivity, and "green" properties. Recent studies have shown that some ILs can match or even exceed the tribological behavior of high-performance lubricants such as PFPEs. This favorable behavior is attributed to the polar nature of ILs, enabling them to physically or chemically adsorb or react to the substrate surface, as well as form wear-resistant surface protective films during sliding.

The main issues concerning the use of ILs as lubricants include corrosion, thermal oxidation, tribochemical reactions, as well as toxicity. These issues can be resolved or minimized through the incorporation of anticorrosion

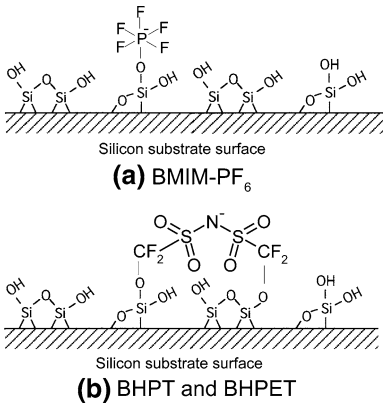


**Fig. 21** Schematic for the attachment of the anions of **a** BMIM-$PF_6$ and **b** BHPT and BHPET to the silicon substrate [29]

additives, as well as the careful selection of cations and anions, which involves a full characterization of its chemical and physical properties and the consideration of potential decomposition or reactivity mechanisms.

Since electrical conductivity is the main characteristic that distinguishes ILs from conventional high-performance lubricants, additional studies relating tribological and electrical behavior of various IL-substrate systems are needed in order to expand the applicability of ILs. In addition, further investigations of the molecular mechanisms that account for the lubricating properties of ILs are necessary to systematically identify the optimal cation–anion combinations for various substrates.

## References


1. Bhushan, B.: Tribology and Mechanics of Magnetic Storage Devices, 2nd edn. Springer, New York (1996)
2. Bhushan, B.: Tribology Issues and Opportunities in MEMS. Kluwer Academic, Dordrecht, The Netherlands (1998)
3. Bhushan, B.: Handbook of Micro/Nanotribology, 2nd edn. CRC, Boca Raton, FL (1999)
4. Bhushan, B.: Introduction to Tribology. Wiley, New York (2002)
5. Bhushan, B.: Nanotribology and Nanomechanics—An Introduction, 2nd edn. Springer-Verlag, Heidelberg, Germany (2008)
6. Bhushan, B.: Springer Handbook of Nanotechology, 3rd edn. Springer-Verlag, Heidelberg, Germany (2010)
7. Bhushan, B., Lee, H., Chaparala, S.C., Bhatia, V.: Nanolubrication of sliding components in adaptive optics used in microprojectors. Appl. Surf. Sci. **256**, 7545–7558 (2010)
8. Henck, S.A.: Lubrication of digital micromirror devices. Tribol. Lett. **3**, 239–247 (1997)
9. Douglass, M.R.: Lifetime estimates and unique failure mechanisms of the digital micromirror device (DMD). In: Proceedings of the 36th Annual International Reliability Physics Symposium, pp. 9–16. IEEE Press, New Jersey (1998)
10. Sulouff, R.E.: MEMS opportunities in accelerometers and gyros and the microtribology problems limiting commercialization. In: Bhushan, B. (ed.) Tribology Issues and Opportunities in MEMS, pp. 109–119. Kluwer Academic, Dordrecht, The Netherlands (1998)
11. Vettiger, P., Brugger, J., Despont, M., Dreschler, U., Durig, U., Haberle, W., Lutwyche, M., Rothuizen, H., Stuz, R., Widmer, R., Binnig, G.: Ultrahigh density, high data rate NEMS-based AFM data storage system. Microelectron. Eng. **46**, 11–17 (1999)
12. Bhushan, B., Kwak, K.J., Palacio, M.: Nanotribology and nanomechanics of AFM probe-based data recording technology. J. Phys. Condens. Matter **20**, 365207-1-34 (2008)
13. Liu, H., Bhushan, B.: Nanotribological characterization of molecularly thick lubricant films for applications to MEMS/NEMS by AFM. Ultramicroscopy **97**, 321–340 (2003)
14. Tao, Z., Bhushan, B.: Bonding, degradation and environmental effects on novel perfluoroether lubricants. Wear **259**, 1352–1361 (2005)
15. Bhushan, B., Tao, Z.: Lubrication of advanced metal evaporated tapes using novel perfluoroether lubricants. Microsyst. Technol. **12**, 579–587 (2006)
16. Rooney, D.W., Seddon, K.R.: Ionic liquids. In: Wypych, G. (ed.) Handbook of Solvents. ChemTec Publishing, Toronto (2001)
17. Kinzig, B.J., Sutor, P., Sawyer, W.G., Rennie, A., Dickrell, P., Gresham, J.: Novel ionic liquid lubricants for aerospace and MEMS. In: ASME World Tribology Congress Proceedings, WTC2005-63744, pp. 509–510. ASME Press, New York (2005)
18. Keskin, S., Kayrak-Talay, D., Akman, U., Hortacsu, O.: A review of ionic liquids towards supercritical fluid applications. J. Supercrit. Fluids **43**, 150–180 (2007)
19. Zhao, H.: Innovative applications of ionic liquids as "green" engineering liquids. Chem. Eng. Commun. **193**, 1660–1677 (2006)
20. Hough, W.L., Rogers, R.D.: Ionic liquids then and now: from solvents to materials to active pharmaceutical ingredients. Bull. Chem. Soc. Jpn. **80**, 2262–2269 (2007)
21. Torimoto, T., Tsuda, T., Okazaki, K., Kuwabata, S.: New frontiers in materials science opened by ionic liquids. Adv. Mater. **22**, 1196–1221 (2010)
22. Ye, C., Liu, W., Chen, Y., Yu, L.: Room-temperature ionic liquids: a novel versatile lubricant. Chem. Commun. **2001**, 2244–2245 (2001)
23. Liu, W., Ye, C., Gong, Q., Wang, H., Wang, P.: Tribological performance of room-temperature ionic liquids as lubricant. Tribol. Lett. **13**, 81–85 (2002)
24. Liu, W., Ye, C., Chen, Y., Ou, Z., Sun, D.C.: Tribological behavior of sialon ceramics sliding against steel lubricated by fluorine-containing oils. Tribol. Int. **35**, 503–509 (2002)
25. Phillips, B.S., Zabinski, J.S.: Ionic liquid lubrication effects on ceramics in a water environment. Tribol. Lett. **17**, 533–541 (2004)
26. Nainaparampil, J.J., Phillips, B.S., Eapen, K.C., Zabinski, J.S.: Micro-nano behavior of DMBI-$PF_6$ ionic liquid nanocrystals: large and small-scale interfaces. Nanotechnology **16**, 2474–2481 (2005)
27. Bhushan, B., Palacio, M., Kinzig, B.: AFM-based nanotribological and electrical characterization of ultrathin wear-resistant ionic liquid films. J. Colloid Interface Sci. **317**, 275–287 (2008)
28. Palacio, M., Bhushan, B.: Ultrathin wear-resistant ionic liquid films for novel MEMS/NEMS applications. Adv. Mater. **20**, 1194–1198 (2008)
29. Palacio, M., Bhushan, B.: Molecularly thick dicationic liquid films for nanolubrication. J. Vac. Sci. Technol. A **27**, 986–995 (2009)
30. Bermudez, M.D., Jimenez, A.E., Sanes, J., Carrion, F.J.: Ionic liquids as advanced lubricant fluids. Molecules **14**, 2888–2908 (2009)
31. Minami, I.: Ionic liquids in tribology. Molecules **14**, 2286–2305 (2009)
32. Zhou, F., Liang, Y., Liu, W.: Ionic liquid lubricants: designed chemistry for engineering applications. Chem. Soc. Rev. **38**, 2590–2599 (2009)

33. Van Valkenburg, M.E., Vaughn, R.L., Williams, M., Wilkes, J.S.: Ionic liquids as thermal fluids. Electrochem. Soc. Proc. 2002-19, 112–123 (2002)
34. Kinzig, B.J., Sutor, P.: Ionic liquids: novel lubrication for air and space. Phase I Final Report for AFOSR/NL. Surfaces Research and Applications, Inc., Lenexa, KS (2005)
35. Chambers, R.G.: Electrons in Metals and Semiconductors. Chapman and Hall, London (1990)
36. Qu, J., Truhan, J.J., Dai, S., Luo, H., Blau, P.J.: Ionic liquids with ammonium cations as lubricants or additives. Tribol. Lett. **22**, 207–214 (2006)
37. Merck Ionic Liquids Database, Darmstadt, Germany. http://ildb.merck.de/ionicliquids/en/startpage.htm
38. Z-TETRAOL Data Sheet. Solvay Solexis Inc., Thorofare, NJ
39. Reich, R.A., Stewart, P.A., Bohaychick, J., Urbanski, J.A.: Base oil properties of ionic liquids. Lubr. Eng. **49**, 16–21 (2003)
40. Wang, H., Lu, Q., Ye, C., Liu, W., Cui, Z.: Friction and wear behaviors of ionic liquid of alkylimidazolium hexafluorophosphates as lubricants for steel/steel contacts. Wear **256**, 44–48 (2004)
41. Kabo, G.J., Blokhin, A.V., Paulechka, Y.U., Kabo, A.J., Shymanovich, M.P., Magee, J.W.: Thermodynamic properties of 1-butyl-3-methylimidazolium hexafluorophosphate in the condensed state. J. Chem. Eng. Data **49**, 453–461 (2004)
42. Frez, C., Diebold, G.J., Tran, C.D., Yu, S.: Determination of thermal diffusivities, thermal conductivities and sound speed of room-temperature ionic liquids by the transient grating technique. J. Chem. Eng. Data **51**, 1250–1255 (2006)
43. Carda-Broch, S., Berthod, A., Armstrong, D.W.: Solvent properties of the 1-butyl-3-methylimidazolium hexafluorophosphate ionic liquid. Anal. Bioanal. Chem. **375**, 191–199 (2003)
44. Ye, C., Liu, W., Chen, Y., Ou, Z.: Tribological behavior of Dy-sialon ceramics sliding against $Si_3N_4$ under lubrication of fluorine-containing oils. Wear **253**, 579–584 (2002)
45. Forsyth, M., Neil, W.C., Howlett, P.C., Macfarlane, D.R., Hinton, B.R.W., Rocher, N., Kemp, T.F., Smith, M.E.: New insights into the fundamental chemical nature of ionic liquid film formation on magnesium alloy surfaces. ACS Appl. Mater. Interfaces **1**, 1045–1052 (2009)
46. Sanes, J., Carrion, F.J., Bermudez, M.D., Martinez-Nicolas, G.: Ionic liquids as lubricants of polystyrene and polyamide-6 contacts. Preparation and properties of new polymer-ionic liquid dispersions. Tribol. Lett. **21**, 121–133 (2006)
47. Carrion, F.J., Sanes, J., Bermudez, M.D.: Effect of ionic liquid on the structure and tribological properties of polycarbonate-zinc oxide nanodispersion. Mater. Lett. **61**, 4531–4535 (2007)
48. Omotowa, B.A., Phillips, B.S., Zabinski, J.S., Shreeve, J.M.: Phosphazene-based ionic liquids: synthesis, temperature-dependent viscosity, and effect as additives in water lubrication of silicon nitride ceramics. Inorg. Chem. **43**, 5466–5471 (2004)
49. Bermudez, M.D., Jimenez, A.E.: Surface interactions and tribochemical processes in ionic liquid lubrication of aluminum-steel contacts. Int. J. Surf. Sci. Eng. **1**, 100–110 (2007)
50. Zhao, Z., Shao, Y., Wang, T., Feng, D., Liu, W.: Corrosion resistance of steel in ethanol containing ionic liquid salts. Corrosion **65**, 674–680 (2009)
51. Caporali, S., Ghezzi, F., Giorgetti, A., Lavacchi, A., Tolstogouzov, A., Bardi, U.: Interaction between an imidazolium based ionic liquid and the AZ91D magnesium alloy. Adv. Eng. Mater. **9**, 185–190 (2007)
52. Liu, X., Zhou, F., Liang, Y., Liu, W.: Benzotriazole as additive for ionic liquid lubricant: one pathway towards actual application of ionic liquids. Tribol. Lett. **23**, 191–196 (2006)
53. Yu, B., Zhou, F., Pang, C., Wang, B., Liang, Y., Liu, W.: Tribological evaluation of $\alpha,\omega$-diimidazoliumalkylene hexafluorophosphate ionic liquid and benzotriazole as additive. Tribol. Int. **41**, 797–801 (2008)
54. Minami, I., Kamimura, H., Mori, S.: Thermo-oxidative stability of ionic liquids as lubricating fluids. J. Synth. Lubr. **24**, 135–147 (2007)
55. Lu, Q., Wang, H., Ye, C., Liu, W., Xue, Q.: Room temperature ionic liquid 1-ethyl-3-hexylimidazolium-bis(trifluoromethylsulfonyl)-imide as lubricant for steel-steel contact. Tribol. Int. **37**, 547–552 (2004)
56. Kamimura, H., Kubo, T., Minami, I., Mori, S.: Effect and mechanism of additives for ionic liquids as new lubricants. Tribol. Int. **40**, 620–625 (2007)
57. Phillips, B.S., John, G., Zabinski, J.S.: Surface chemistry of fluorine containing ionic liquids on steel substrates at elevated temperatures using Mössbauer spectroscopy. Tribol. Lett. **26**, 85–91 (2007)
58. Swatlowski, R.P., Holbrey, J.H., Rogers, R.D.: Ionic liquids are not always green: hydrolysis of 1-butyl-3-methylimidazolium hexafluorophosphate. Green Chem. **5**, 361–363 (2003)
59. Wasserscheid, P., van Hal, R., Bössman, A.: 1-n-Butyl-3-methylimidazolium ([bmim]) octylsulfate—an even "greener" ionic liquid. Green Chem. **4**, 400–404 (2002)
60. Bernot, R.J., Brueseke, M.A., Evans-White, M.A., Lamberti, G.A.: Acute and chronic toxicity of imidazolium-based ionic liquids on *Daphnia magna*. Environ. Toxicol. Chem. **24**, 87–92 (2005)
61. Harrison, B., Czerw, R., Konchady, M.S., Pai, D.M., Lopatka, M.W., Jones, P.B.: Ionic liquids incorporating nanomaterials as lubricants for harsh environments. In: Proceedings of the ASME Materials Division, pp. 405–410. ASME Press, New York (2005)
62. Yu, B., Liu, Z., Zhou, F., Liu, W., Liang, Y.: A novel lubricant additive based on carbon nanotubes for ionic liquids. Mater. Lett. **62**, 2967–2969 (2008)
63. Kondo, H.: Protic ionic liquids with ammonium salts as lubricants for magnetic thin film media. Tribol. Lett. **31**, 211–218 (2008)
64. Zhu, M., Yan, J., Mo, Y., Bai, M.: Effect of the anion on the tribological properties of ionic liquid nano-films on surface-modified silicon wafers. Tribol. Lett. **29**, 177–183 (2008)
65. Xie, G., Wang, Q., Si, L., Liu, S., Li, G.: Tribological characterization of several silicon-based materials under ionic-liquid lubrication. Tribol. Lett. **36**, 247–257 (2009)
66. Nooruddin, N.S., Wahlbeck, P.G., Carper, W.R.: Semi-empirical molecular modeling of ionic liquid tribology: ionic liquid-hydroxylated silicon surface interactions. Tribol. Lett. **36**, 147–156 (2009)
67. Perkin, S., Albrecht, T., Klein, J.: Layering and shear properties of an ionic liquid, 1-ethyl-3-methylimidazolium ethylsulfate, confined to nano-films between mica surfaces. Phys. Chem. Chem. Phys. **12**, 1243–1247 (2010)
68. Ueno, K., Kasuya, M., Watanabe, M., Mizukami, M., Kurihara, K.: Resonance shear measurement of nanoconfined ionic liquids. Phys. Chem. Chem. Phys. **12**, 4066–4071 (2010)
69. Xie, G., Luo, J., Guo, D., Liu, S.: Nanoconfined ionic liquids under electric fields. Appl. Phys. Lett. **96**, 043112 (2010)
70. Manini, N., Cesaratto, M., Del Popolo, M.G., Ballone, P.: Mesophases in nearly 2-D room-temperature ionic liquids. J. Phys. Chem. B **113**, 15602–15609 (2009)
71. Mazyar, O.A., Jennings, G.K., McCabe, C.: Frictional dynamics of alkylsilane monolayers on $SiO_2$: effect of 1-n-butyl-3-methylimidazolium nitrate as a lubricant. Langmuir **25**, 5103–5110 (2009)
72. Anderson, J.L., Ding, R., Ellern, A., Armstrong, D.W.: Structure and properties of high stability germinal dicationic ionic liquids. J. Am. Chem. Soc. **127**, 593–604 (2005)
73. Payagala, T., Huang, J., Breitbach, Z.S., Sharma, P.S., Armstrong, D.W.: Unsymmetrical dicationic ionic liquids:

manipulation of physicochemical properties using specific structural architectures. Chem. Mater. **19**, 5848–5850 (2007)
74. Mo, Y., Yu, B., Zhao, W., Bai, M.: Microtribological properties of molecularly thin carboxylic acid functionalized imidazolium ionic liquid film on single-crystal silicon. Appl. Surf. Sci. **255**, 2276–2283 (2008)
75. Mo, Y., Zhao, W., Zhu, M., Bai, M.: Nano/microtribological properties of ultrathin functionalized imidazolium wear-resistant ionic liquid films on single crystal silicon. Tribol. Lett. **32**, 143–151 (2008)
76. Zhao, W., Mo, Y., Pu, J., Bai, M.: Effect of cation on micro/nanotribological properties of ultra-thin ionic liquid films. Tribol. Int. **42**, 828–835 (2009)
77. Zhao, W., Zhu, M., Mo, Y., Bai, M.: Effect of anion on micro/nanotribological properties of ultra-thin imidazolium ionic liquid films on silicon wafer. Colloid Surf. A **332**, 78–83 (2009)
78. Zhu, M., Mo, Y., Zhao, W., Bai, M.: Micro/macrotribological properties of several nano-scale ionic liquid films on modified silicon wafers. Surf. Interface Anal. **41**, 205–210 (2009)
79. Palacio, M., Bhushan, B.: Surface potential and resistance measurements for detecting wear of chemically-bonded and unbonded molecularly-thick perfluoroether lubricant films using atomic force microscopy. J. Colloid Interface Sci. **315**, 261–269 (2007)
80. Bhushan, B., Goldade, A.V.: Kelvin probe microscopy measurements of surface potential change under wear at low loads. Wear **244**, 104–117 (2000)
81. Lodge, R.A., Bhushan, B.: Effect of physical wear and triboelectric interaction on surface charge as measured by Kelvin probe microscopy. J. Colloid Interface Sci. **310**, 321–330 (2007)
82. Valkenberg, M.H., de Castro, C., Holderich, W.F.: Immobilization of ionic liquids on solid supports. Green Chem. **4**, 88–93 (2002)
83. Zhang, L., Zhang, Q., Li, J.: Electrochemical behaviors and spectral studies of ionic liquid (1-butyl-3-methylimidazolium tetrafluoroborate) based on sol-gel electrode. J. Electroanal. Chem. **603**, 243–248 (2007)